

Development of Optimal Concrete Sealant Techniques

PB2000-102763



FINAL REPORT No. FHWA/OH-99/007

May, 1999

Submitted to

The Ohio Department of Transportation

by

Robert L. Mullen, Philip C. Perdikaris and Alec B. Patton

Department of Civil Engineering

Case Western Reserve University

Cleveland, Ohio 44106

Prepared in cooperation with the Ohio Department of Transportation and the U.S. Department of Transportation, Federal Highway Administration

The content of this report reflects the views of the authors who are responsible for the facts and the accuracy of the data presented herein. The contents do not necessarily reflect the official views or policies of the Ohio Department of Transportation or the Federal Highway Administration. This report does not constitute a standard, specification or regulation.

REPRODUCED BY:
U.S. Department of Commerce
National Technical Information Service
Springfield, Virginia 22161



1. Report No. FHWA/OH-99/007	2. Government Accession No.	3. Recipient's Catalog No.	
4. Title and Subtitle DEVELOPMENT OF OPTIMAL CONCRETE SEALANT TECHNIQUES		5. Report Date May, 1999	
		6. Performing Organization Code	
7. Author(s) Robert L. Mullen, Philip C. Perdikaris		8. Performing Organization Report No.	
9. Performing Organization Name and Address Case Western Reserve University Department of Civil Engineering Cleveland, OH 44106-7201		10. Work Unit No. (TRAIS)	
		11. Contract or Grant No. State Job No. 14619(0)	
12. Sponsoring Agency Name and Address Ohio Department of Transportation 1600 West Broad Street Columbus, OH 43223		13. Type of Report and Period Covered Final Report	
		14. Sponsoring Agency Code	
15. Supplementary Notes Prepared in cooperation with the U.S. Department of Transportation, Federal Highway Administration			
16. Abstract <p>Though concrete coatings and sealants have been known to prolong the service life of concrete highway structures for some time, ignorance of the effect that moisture encapsulation has on the performance of such surface treatments persists. This study investigates the phenomenon of moisture encapsulation and how concrete sealants and coatings influence concrete freeze/thaw durability and moisture migration.</p> <p>In this project several commercially available concrete coatings are applied to concrete cylinders of two sizes. The parameters of the study include curing duration and environment for the concrete, air drying time before coating and coated surface area. Based on freeze/thaw durability tests (150 cycles) in air of a group of specimens cast with Class "C" structural concrete (4,000 psi or 27.6 MPa) it is concluded that encapsulation of moisture does not contribute to freeze/thaw degradation. Subsequent freeze/thaw cycling of another group of cylinders of lower compressive strength in water demonstrates that coatings do reduce damage due to weathering. Also, it is concluded that no benefits are obtained by leaving portions of the surface area uncoated to insure "breathability" of the concrete. Furthermore, the important parameter of moisture concentration can be readily and reliably determined by measuring the relative humidity in concrete. A Finite Element Method computer model based on linear diffusion theory is found to adequately predict the drying behavior of concrete treated with relatively impermeable coatings. Nevertheless, it is determined that the process of diffusion alone is insufficient to describe the movement of water in concrete.</p>			
17. Key Words Concrete Sealants, Freeze-thaw damage, Concrete durability, Concrete coatings		18. Distribution Statement No Restrictions. This document is available to the public through the National Technical Information Service, Springfield, Virginia 22161	
19. Security Classif. (of this report) Unclassified	20. Security Classif. (of this page) Unclassified	21. No. of Pages	22. Price

Abstract

Though concrete coatings and sealants have been known to prolong the service life of concrete highway structures for some time, ignorance of the effect that moisture encapsulation has on the performance of such surface treatments persists. This study investigates the phenomenon of moisture encapsulation and how concrete sealants and coatings influence concrete freeze/thaw durability and moisture migration.

In this project several commercially available concrete coatings are applied to concrete cylinders of two sizes. The parameters of the study include curing duration and environment for the concrete, air drying time before coating and coated surface area. Based on freeze/thaw durability tests (150 cycles) in air of a group of specimens cast with Class "C" structural concrete (4,000 psi or 27.6 MPa) it is concluded that encapsulation of moisture does not contribute to freeze/thaw degradation. Subsequent freeze/thaw cycling of another group of cylinders of lower compressive strength in water demonstrates that coatings do reduce damage due to weathering. Also, it is concluded that no benefits are obtained by leaving portions of the surface area uncoated to insure "breathability" of the concrete. Furthermore, the important parameter of moisture concentration can be readily and reliably determined by measuring the relative humidity in concrete. A Finite Element Method computer model based on linear diffusion theory is found to adequately predict the drying behavior of concrete treated with relatively impermeable coatings. Nevertheless, it is

determined that the process of diffusion alone is insufficient to describe the movement of water in concrete.

ACKNOWLEDGMENTS

This project was sponsored by the Ohio Department of Transportation, and additional financial support was furnished by a Richard W. Sicka Fellowship (established by Mrs. Walter Sicka), both of whom the authors wishes to thank for there support.

PROTECTED UNDER INTERNATIONAL COPYRIGHT
ALL RIGHTS RESERVED.
NATIONAL TECHNICAL INFORMATION SERVICE
U.S. DEPARTMENT OF COMMERCE

Reproduced from
best available copy. 

The contents of this report reflect the views of the authors who are responsible for the facts and the accuracy of the data presented herein. The contents do not necessarily reflect the official views or policies of the Ohio Department of Transportation or the Federal Highway Administration. This report does not constitute a standard, specification or regulation.

TABLE OF CONTENTS

ABSTRACT	ii
ACKNOWLEDGMENTS	iv
TABLE OF CONTENTS	v
LIST OF FIGURES	vii
LIST OF TABLES	x
CHAPTER ONE: INTRODUCTION	1
1.1 Statement of the Problem	1
1.2 Objective and Scope of Study	3
1.3 Literature Review	4
1.3.1 Freeze/Thaw Durability	4
1.3.2 Diffusion of Water	6
1.3.3 Concrete Coatings	11
CHAPTER TWO: EXPERIMENTAL PROGRAM	14
2.1 Introduction	14
2.2 Task 1 - Investigation of Moisture Encapsulation	14
2.3 Task 2 - Measurement of Moisture Concentration	21
2.4 Task 3 - Freeze/Thaw Durability	23
2.5 Task 4 - Computer Modeling of Diffusion	26

CHAPTER THREE: DISCUSSION OF RESULTS	28
3.1 Task 1 - Investigation of Moisture Encapsulation	28
3.2 Task 2 - Measurement of Moisture Concentration	34
3.3 Task 3 - Freeze/Thaw Durability	38
3.4 Task 4 - Computer Modeling of Diffusion	56
3.4.1 Diffusion in Uncoated Concrete	56
3.4.2 Diffusion in Coated Concrete	61
CHAPTER FOUR: CONCLUSIONS	65
4.1 Summary and Conclusions	65
4.2 Suggestions for Future Work	67
APPENDIX A: REFERENCES	69

LIST OF FIGURES

Figure 2.1	Climate Control Room	17
Figure 2.2	Interior of Climate Control Room with Coated Specimens and Control Cylinder with Thermocouple	18
Figure 2.3	Typical Freeze/Thaw Cycle Temperature Variation	20
Figure 3.1	Average Compressive Strength Test Results Depicting Overall Coating Performance	30
Figure 3.2	Average Compressive Strength Test Results For Each of the Parameters	31
Figure 3.3	Cross-Section of Specimen Coated with Coating II, After 150 Freeze/Thaw Cycles	33
Figure 3.4	Uncoated Specimen, Not Subjected to Any Freeze/Thaw Cycling	33
Figure 3.5	Percent Mass Loss of Drying 6 x 12 in. Concrete Cylinder in Humidity Experiment	36
Figure 3.6	Humidity Measurements in 6 x 12 in. Concrete Cylinder at Radial Distances of 0, 1.5 and 2 in.	36
Figure 3.7	Distribution of Moisture Within Specimen	37
Figure 3.8	Volume/Concentration Curve for 6 x 12 in. (15.2 x 30.5 cm) Specimen	37
Figure 3.9	Uncoated Specimens (A-U, B-U and C-U)	39
Figure 3.10	Specimens Cured Outside and Coated with Coating I (0-I, 1/4-I and 1-I)	39
Figure 3.11	Specimens Cured Inside and Coated with Coating I (1-I-A, 1-I-B and 1-I-C)	40
Figure 3.12	Specimens Cured Inside and Coated with Coating I (0-I-A, 0-I-B and 0-I-C)	40

Figure 3.13 Specimens Cured Inside and Coated with Coating I (1/4-I-A, 1/4-I-B and 1/4-I-C)	41
Figure 3.14 Specimens Cured Outside and Coated with Coating II (1-II, 1/4-II and 0-II)	41
Figure 3.15 Specimens Cured Inside and Coated with Coating II (1-II-A, 1-II- B and 1-II-C)	42
Figure 3.16 Specimens Cured Inside and Coated with Coating II (0-II-A, 0-II-B and 0-II-C)	42
Figure 3.17 Specimens Cured Inside and Coated with Coating II (1/4-II-A, 1/4-II-B and 1/4-II-C)	43
Figure 3.18 Specimen Cured Outside and Coated with Coating III (0-III)	43
Figure 3.19 Specimens Cured Inside and Coated with Coating III (1-III-A, 1-III-B and 1-III-C)	44
Figure 3.20 Specimens Cured Inside and Coated with Coating III (0-III-A, 0-III-B and 0-III-C)	44
Figure 3.21 Specimens Cured Inside and Coated with Coating III (1/4-III-A, 1/4-III-B and 1/4-III-C)	45
Figure 3.22 Specimens Cured Outside and Coated with Coating IV (1-IV, 1/4-IV and 0-IV)	45
Figure 3.23 Specimens Cured Inside and Coated with Coating IV (1-IV-A, 1-IV-B and 1-IV-C)	46
Figure 3.24 Specimens Cured Inside and Coated with Coating IV (0-IV-A, 0-IV-B and 0-IV-C)	46
Figure 3.25 Specimens Cured Inside and Coated with Coating IV (1/4-IV-A, 1/4-IV-B and 1/4-IV-C)	47

Figure 3.26	Mass Loss Prediction of Computer Diffusion Model Compared to Experimental Data of an Uncoated 15.2 x 30.5 cm (6 x 12 in.) Concrete Cylinder	58
Figure 3.27	Predicted % Mass Loss Values of an Uncoated 15.2 x 30.5 cm Concrete Cylinder for Different Number of Elements	59
Figure 3.28	Mass Loss Prediction Compared to Experimental Data from Specimen Coated with Coating I	62
Figure 3.29	Mass Loss Prediction Compared to Experimental Data from Specimen Coated with Coating II	63
Figure 3.30	Mass Loss Prediction Compared to Experimental Data from Specimen Coated with Coating III	63
Figure 3.31	Mass Loss Prediction Compared to Experimental Data from Specimen Coated with Coating IV	64

LIST OF TABLES

Table 2.1 Concrete Sealants Used in Task 1	15
Table 2.2 Parameters For Task 1	16
Table 2.3 Climate Data: Freeze/Thaw Cycles	19
Table 2.4 Climate Data: Average Temperature Change (ΔT) in a Freeze/Thaw Cycle	19
Table 2.5 Parameters for Task 3 Concrete Batch 1	24
Table 2.6 Parameters for Task 3 Concrete Batch 2	25
Table 3.1 Compressive Strength Test Results on 6 x 12 in. (15.2 x 30.5 cm) Cylinders from Task 1 (1,000psi = 6.9 MPa)	29
Table 3.2 Resonance Frequency Test Results from Task 1	32
Table 3.3 Damage Data for Task 3	48
Table 3.4 Average Spalled Concrete Area as % of Total Surface Area for Different Parameter Categories	50
Table 3.5 Compressive Strength of Selected Concrete Cylinders	52
Table 3.6 Overall Compressive Strength Data for Each Parameter Category	53
Table 3.7 Dynamic Modulus, E_d , of Selected Concrete Cylinders	54
Table 3.8 Dynamic Modulus and Compressive Strength Values in the Second Batch of Concrete	55
Table 3.9 Free Water Values for Saturated Concrete	56
Table 3.10 Reported Values for Diffusion Coefficient of Concrete	57
Table 3.11 Average Coating Thickness and Diffusion Coefficient	62

CHAPTER ONE

INTRODUCTION

1.1 Statement of the Problem

The problem of deterioration of reinforced concrete highway structures due to the combined effects of chloride ion intrusion and weathering as a result of cyclic freezing and thawing is well known. Application of a protective coating on concrete elements is one of the methods used to mitigate the deleterious effects of a harsh climate. The term *concrete coating* refers to such a surface treatment that forms a film on the concrete surface and at most penetrates insignificantly into the concrete. The coating with a thickness ranging from 25 μm to 1 mm (Zemajtis and Weyers, 1995) restricts the diffusion of chloride ions and water into the concrete. Due to their relatively low cost, concrete sealants and coatings present an attractive option for prolonging the service life of a concrete structural element, be it a substructural element such as a pier, abutment, and wall or part of the superstructure such as a girder, a median, walkway or parapet of a bridge deck.

The utility of such coatings, however, may be overestimated. In order to allow timely completion of the construction of concrete highway structures, the coating is applied soon after the form-work is stripped. While undoubtedly convenient and seemingly cost-effective, this practice may result in encapsulation of moisture within the concrete member. This trapped moisture may then lead to undesirable alterations in coating appearance, earlier degradation of the coating and even eventual spalling of

the concrete by giving rise to degenerative forces, "...such as excessive vapor pressure, escalated freeze-thaw damage, and crystal pressure" (Reedy, 1986). As Reedy explained, as the temperature falls, moisture in vapor form migrates in the direction of the coating, and then changes to liquid form at the dew point. As liquids are capable of creating a solution, water soluble material in the concrete is carried along the path the water takes. When the temperature is sufficiently low, the liquid converts into ice and expands causing freeze-thaw damage at the water's destination, namely at the edge of the vapor barrier. The water in the pores of the cement paste also expands as it freezes. If the necessary volume exceeds the space available, then the excess water is driven away by the pressure resulting from the water's expansion. "The magnitude of this hydraulic pressure depends on the permeability of the cement paste, the degree of saturation, the distance to the nearest unfilled void, and the rate of freezing" (Detwiler et al., 1989). Finally, during the thawing process, the moisture eventually returns to its vapor state and loses its ability to hold solubles, leaving them behind in crystalline form.

In order to mitigate this suspected harmful phenomenon of encapsulation, current O.D.O.T. practice (inter-office communication between B.D. Hanhiammi and D.W. Leake, 1993) recommends that one quadrant of the vertical surface of a bridge pier be left uncoated. This obviously ameliorates the effectiveness of the coating. "Breathability" of the concrete is insured by depriving a substantial portion of its surface of the benefits of a protective barrier. It is ironic that such a practice should be

warranted, as it places one in the position of withholding the application of the coating that is supposed to prevent damage because it itself may cause harm!

1.2 Objective and Scope of Study

It is important to establish whether or not encapsulation of moisture is an actual phenomenon, and if so, whether it is as serious as is feared by some in the bridge engineering community. If it is a concern, determination of the most favorable combination of coating parameters is needed. For example, the time of application, type of coating, and the optimal surface area to be treated have to be determined. Furthermore, a method is needed to obtain moisture concentration measurements, as moisture concentration is a driving force behind freeze-thaw concrete deterioration and coating failure. One should be able to in situ monitor this type of behavior as well as predict it with the aid of a computer model.

The objectives of this research are:

- a. Establish if moisture encapsulation really occurs in coated concrete.
- b. Determine the effectiveness of coatings in mitigating freeze/thaw damage.
- c. Develop an experimental procedure for determining the moisture concentration in concrete.
- d. Model moisture migration in coated and uncoated concrete with a diffusion computer program.

Chapter Two describes the experimental setup. The experimental results, including the measurements on compressive strength, resonant frequency, relative

humidity, damage evaluation, and mass loss and the predicted behavior, based on a computer diffusion model, are presented in Chapter Three. Chapter Four is devoted to the conclusions garnered from this research and includes suggestions for future work.

1.3 Previous Work

1.3.1 Freeze/Thaw Durability

Freezing and thawing has long been known to have a detrimental effect on the durability of concrete. Mechanisms that precipitate freeze/thaw damage were proposed by Neville [1963], Cordon [1966] and Cady [1969]. However, factors affecting freeze/thaw durability remained qualitative for a long time. A comprehensive mathematical model that accounted for heat conduction, moisture diffusion, pore pressures, permeability, and the effect of superimposed stresses due to applied loads was not available until Bazant et al. formulated one in 1988.

In order to minimize the degradation in concrete that is perpetrated by cold and warm temperature fluctuations, two basic preventive measures are taken to prolong concrete service life. The first is air entrainment and the second is sealing or coating the concrete surface. Both deal with manipulating the flow of moisture.

The crucial need for a suitable air-void system in concrete subjected to the unavoidable temperature cycling of hostile climates has been known for about 50 years. In 1949 Powers suggested that an evenly distributed system of air voids in the cement matrix of concrete would result in significant reduction of internal stresses

caused by the expansion of frozen pore water. Inadequate dispersion of air voids or insufficient air entrainment may allow stresses that could result in cracking and/or spalling of the concrete. Powers' hydraulic pressure theory was expanded by Helmuth [1960] into an osmotic pressure theory. Good quality materials and well-made concrete were discovered to be insufficient to ensure proper performance and as Cook [1952] asserted, concrete "...will not ordinarily withstand the exposure of more than one winter unless the concrete contains proper amounts of entrained air."

Determination of the best air-void parameters for air entrainment is vital. Therefore, a reliable method for estimation of these parameters has been the subject of considerable research. Sommer [1979] outlined a method for determination of the particulars of an air-void system with microscopy, and discussed the influence the quality of samples have on air-void analysis. The air-void structure of hardened concrete is customarily measured on 20 mm thick or very thin 20 μm thick polished sections (Detwiler et al., 1989), using the linear traverse or modified point-count method described by ASTM Standard C 457, "Standard Practice for Microscopical Determination of Air-Void Content and Parameters of the Air-Void System in Hardened Concrete". The effect of varying cross-sectional analysis areas was considered by Sandstrom [1991]. A theoretical evaluation of air-void analysis using stereological methods was conducted by Aarne [1995], who claimed that precision of the analysis could be refined with the introduction of a correction factor to offset errors inherent in standard air-void measurements.

However, even an optimal air-void structure will not prevent freeze/thaw damage if concrete contains so much evaporable water that there is not enough space to accommodate expansion of the water as it freezes. Fagerlund [1977] proposed a test that could establish the critical degree of saturation and predict the frost resistance of a given concrete sample by comparing the critical and the actual level of saturation at a given time. However, Detwiler et al. [1989] cautioned that this test, as well as other standard tests such as ASTM C 666, "Resistance of Concrete to Rapid Freezing and Thawing", ASTM C 671, "Critical Dilation of Concrete Specimens Subjected to Freezing," and ASTM C 682, "Standard Recommended Practice for Evaluation of Frost Resistance of Coarse Aggregates in Air-Entrained Concrete by Critical Dilation Procedures", merely assess a property of concrete. They questioned the usefulness of such tests because results from particular tests may not provide a valid comparison for the in service behavior of concrete. For example, conventional freeze/thaw tests are too rapid to account for the mechanism of ice accretion, which only becomes a factor in concrete failure when concrete has been frozen for considerable periods of time. The inclusion of an examination of the microstructure of concrete weathered in the lab as well as in natural conditions was suggested as a remedy for this deficiency. Bakharev and Struble [1995] also examined the microstructure of concrete exposed to freeze/thaw and used their observations to link cracking to concrete permeability.

1.3.2 Diffusion of Water

In order to model the behavior of moisture within concrete, diffusion theory must be used in conjunction with experimental evidence. *Diffusion* is the process by

which matter is transported from one region of a system to another due to random molecular motion. The basic mathematical theory of the diffusion process is derived from the same equations used to describe the transfer of heat by conduction, as the two processes are analogous in the respect that heat transfer is also due to random molecular motion. Fick [1855] was the first to express diffusion quantitatively by adapting the mathematical equation used for heat conduction.

Diffusion theory is based on the hypothesis that the rate of transfer of the diffusing substance through a unit area of a section is proportional to the concentration gradient, measured normal to the section. This can be otherwise stated as:

$$F = -D \frac{\partial C}{\partial x}, \quad (1.1)$$

where F is the rate of transfer per unit area of the section, C the concentration of the diffusing material, x a spatial coordinate measured along the normal to the surface, and D the coefficient of diffusion having the units of L^2/T . The diffusion coefficient is often assumed to be a constant. This equation is known as Fick's First Law.

If the concentration gradient is only along the x -axis, i.e. the diffusion is one-dimensional, then mass conservation and Fick's First Law result in the fundamental differential equation of diffusion:

$$\frac{\partial C}{\partial t} = D \frac{\partial^2 C}{\partial x^2} \quad (1.2)$$

This is known as Fick's Second Law. Fick's Second Law was also formulated by analogy with the equations of heat transfer derived by Fourier [1822].

Sherwood [1929] was the first to advance the notion that the diffusion process describes the drying process in porous substances. Early work on diffusion in concrete was reported by Pickett [1946] and Carlson [1937], who were primarily concerned with moisture diffusion as it related to shrinkage effects. Pickett surmised that the differential equation for the flow of water in concrete would be a diffusion equation provided the migration of water in concrete was due entirely by diffusion of vapor, the vapor pressure of the water was proportional to the moisture content, and the permeability was independent of the moisture content. He solved a linear diffusion equation. Carlson found that elementary diffusion worked for the first half of a moisture loss curve, but the utility of linear diffusion theory declined thereafter. Penev and Kawamura [1991] concurred and expressed D as a function of a combined variable of space and time (the Boltzmann variable, $\eta = x/t^{1/2}$), and introduced a surface factor to more accurately reflect the boundary conditions.

Lowe et al. [1971] initially attempted to model moisture diffusion in concrete by assuming a constant diffusion coefficient, but conceded that the diffusion coefficient decreased as drying continued, thereby indicating that it was at least partially moisture concentration dependent. It was postulated that "surface retardation" slowed the drying process, and that a slow rate of moisture removal meant that diffusion could not "fully operate". In addition, the drying curves were normalized for specimens of varying size, and size dependence was found not to be a factor affecting moisture loss. However, since the prior studies of Hughes et al. [1966] showed that a single constant

diffusion coefficient was adequate to describe drying at higher temperatures (50 to 90°C), it was concluded that concentration dependence was relatively small, perhaps dominated by other phenomena. The complications arising from adopting a moisture dependent diffusion coefficient were minimized by using a time dependent coefficient. Odler and Barthold [1989] took a different stance altogether, and declared that only at a low relative humidity is water vapor diffusion dominant because capillary condensation in the pores cannot occur. They linked water migration to porosity of concrete, but otherwise limited their description of drying to qualitative observations.

Others also have used a diffusion coefficient that was based on relative humidity or of moisture content, though Wittman et al. [1988] admitted that the direct influence of moisture content and the indirect influence of parameters such as water/cement ratio, curing conditions and age "...have not been studied in detail. Almost no data on the influence of the above parameters are available in the literature." Wittman formulated a model, the so-called "3L-approach", which consisted of a macro, meso, and micro-level to describe the drying process in concrete. The micro-level serves to describe the properties characteristic of cement paste. The meso-level takes into consideration the composite nature of concrete, and the macro-level uses the preceding levels to develop realistic material laws.

Bazant and Najjar [1971] and Sakata [1983] also demonstrated that the diffusion coefficient was affected by the moisture content, at least at the onset of drying. Sakata introduced a "surface factor" along with a nonlinear diffusion theory to

obtain a suitable fit for the experimental data. Wittman et al. [1989] went a step further using numerical analysis of experimental data from moisture loss measurements, and asserted that the diffusion coefficient was strongly related to the water/cement ratio. He declared that Sakata's method underestimates the real moisture content as drying proceeds and suggested that for low moisture contents "...direct and non-destructive observation of the moisture content is necessary." Miao [1988] and Mensi et al. [1988] used the same numerical analysis techniques to determine the influence of temperature on the diffusion coefficient D .

Varying forms of the dependence of D on the moisture content have been used in the literature. A power function of the form

$$D(U) = a_0 + a_1 U^{a_2} \quad (1.3)$$

was suggested by Pihlajavaara [1965], where U is the moisture content and a_i are constants. Mensi et al., on the other hand, proposed an exponential function

$$D(U) = a_0 \exp(a_1 U), \quad (1.4)$$

and a popular S-shaped function was advanced by Bazant and Najjar:

$$D(H) = a_0 \left[a_1 + \frac{1 - a_1}{1 + \left(\frac{1 - H}{1 - a_2} \right)^{a_3}} \right], \quad (1.5)$$

where H is the relative humidity in the pores.

1.3.3 Concrete Coatings

As has been noted before, it is undesirable for excess water to be retained within concrete. As air entrainment is not always sufficient to prevent freeze/thaw degradation, and the drying process in concrete is rather slow, coatings are often used to halt the intrusion of water. But concrete coatings have other uses as well. They are used to prevent the intrusion of chloride ions (especially in marine environments), concrete carbonation, and expansion due to the alkali-silica reaction.

Chloride ions are of concern because of the corrosion they expedite in steel reinforcement. Swamy and Tanikawa [1990], Terro and Hughes [1990], Fukute and Hamada [1990], Zemajtis and Weyers [1995], Weyers et al. [1995], and Fera [1991] have evaluated the performance of several coatings with respect to chloride ion diffusion.

Concrete carbonation is another process that promotes rebar corrosion. Alkaline compounds in the hydrated cement paste react with carbon dioxide to produce carbonates. While not harmful in and of themselves, these chemical reactions cause the pH of the pore water to fall, seriously compromising the protection afforded by the alkaline environment to the steel reinforcement. Diffusion of carbon dioxide into concrete can be slowed with the introduction of coatings, as was shown by Garcia et al. [1990], who developed a testing methodology for this phenomenon. Significant delay of concrete carbonation can be accomplished with the use of the proper impermeable coatings.

If the evaporable water in concrete is above 4%, cement mortar may expand as a result of the alkali-silica reaction, giving rise to potentially harmful stresses. Aggregates that contain siliceous material react with alkalis that originate from seawater or deicing salts and form a gel-like compound. Blight [1990] reported on the efficacy of sealants to maintain concrete at a proper level of desiccation.

There are many types of concrete coatings, reflecting the burgeoning nature of the coatings industry in general. Assistance to the engineer attempting to select the most appropriate one is of paramount value. To reduce confusion, McGill [1990] has crafted a comprehensive report that classifies and describes the various types, and Foscante and Kline [1988], Harwood [1990] and Aldinger [1991] have issued sets of guidelines as to how to go about selecting the best coating for a project. Included are considerations such as required materials and equipment, concrete condition, curing and pretreatment, surface preparation, material mixing and application, climate, inspection, testing, necessary remedial work, safety and environmental concerns.

As useful as coatings are, they are nevertheless no panacea in regard to protecting concrete. Leeming [1990] addressed several causes of coating failure, including loss of adhesion due to poor surface preparation and deposition of soluble materials at the concrete/coating interface, blistering due to capillary or osmotic forces, and coating degradation due to different thermal expansion coefficients of the coating and concrete substrate. Swamy and Tanikawa [1990] discussed the negative effects of tensile stress on coating diffusion resistance as well as the effect of water content of the concrete on adhesion strength. Nguyen et al. [1995] concurred that

water at the interface "...is often the main cause of corrosion, blistering, and disbondment of organic coating/substrate systems." In addition, Nguyen and Leeming acknowledged that methods of testing coatings remained unreliable because coatings are either tested as free films or on a paper substrate along with unusual or contrived relative humidities. Thus, such results may not necessarily directly relate to the performance of coatings in service.

CHAPTER TWO

EXPERIMENTAL PROGRAM

2.1 Introduction

The experimental program is divided into three tasks. In Task 1 a laboratory study was conducted to determine whether moisture encapsulation in concrete contributed to sealant degradation. In Task 2 a technique was developed for the measurement of moisture permeability in a typical concrete specimen. In Task 3 additional laboratory freeze/thaw experiments were carried out on concrete cylinders that were either partially or completely sealed and subsequently immersed in water. In Task 4 a computer program was used to model the behavior of the diffusion of water in uncoated and coated concrete specimens and the theoretical predictions were compared to experimental data.

2.2 Task 1 - Investigation of Moisture Encapsulation

Cylindrical concrete specimens were cast following ASTM Standard C 192, "Practice for Making and Curing Concrete Test Specimens in the Laboratory", using Class C structural concrete (O.D.O.T., 1989). The concrete mix per cubic yard consists of: 1,285 lb (5,718 kN) fine aggregate, 1,630 lb (7,254 kN) coarse aggregate (No. 57 limestone), 600 lb (2,670 kN) type I Portland cement, with a w/c ratio of 0.5 and air entrainment of $6 \pm 2\%$. The target compressive strength was 4,000 psi (27.6

MPa). The concrete was provided by Cuyahoga Concrete, a local ready-mix company.

Sixty of the specimens were cured for 28 days, and sixty for 7 days. The concrete cylinders were subjected to two different curing environments: half of them were cured in 100% relative humidity maintained at 70°F, and the other half were covered with wet burlap and plastic sheets and were cured at room temperature (approximately 70°F) to simulate field curing conditions. In order to account for the effect of surface area to concrete volume ratio two sizes of concrete cylinders were used: 4 x 8 in. (10.2 x 20.3 cm) and 6 x 12 in. (15.2 x 30.5 cm). All cylinders were stripped of their molds 3 days subsequent to casting. After the required curing period was completed, the specimens were allowed to dry in air for 0, 3, 5, 15 and 30 days. Following the air-drying, the entire surface of the specimen was coated with selected sealants.

Three commercially available concrete sealants were used in this phase: a silane penetrant, a penetrating epoxy and a water based epoxy (see Table 2.1). All sealants were applied with a brush after the surface of each specimen was scarified, etched with compressed air, washed, and dried.

Table 2.1
Concrete Sealants Used in Task 1

Designation	Type
Coating I	silane penetrant (non-epoxy)
Coating II	penetrating epoxy
Coating III	water based epoxy

There were five parameters studied in Task 1, as shown in Table 2.2, the type of coating, curing duration, specimen size, curing environment and air drying time before application of the coating. One cylinder was cast for each combination of the above five parameters, resulting in a total of $3 \times 2 \times 2 \times 2 \times 5 = 120$ concrete specimens.

Table 2.2
Parameters For Task 1

Coating	1. I 2. II 3. III
Curing Duration	1. 7 Days 2. 28 Days
Specimen Size	1. 4 x 8 in. Cylinder 2. 6 x 12 in. Cylinder
Curing Environment	1. Curing Room with 100% RH 2. Specimens covered with wet burlap and plastic
Air Drying Time Before Application	1. 0 Days 2. 3 Days 3. 5 Days 4. 15 Days 5. 30 Days

The specimens were then placed in a Hotpack Model #883-M Portable Controlled Environment Walk-In Room (see Figure 2.1), and were subjected to 150 freeze/thaw cycles, which were controlled by a thermocouple embedded in a 6 x 12 in. concrete cylinder at its geometrical center (see Figure 2.2), and connected to a computer-data acquisition and control system.

In order to determine the relationship between field and laboratory tests, climate data was analyzed for recent winters in the northern and southern regions in the State of Ohio (EarthInfo, 1995). The number of freeze/thaw cycles in a winter were obtained and shown in Table 2.3. As can be seen, the number of cycles appears relatively constant for each season.



Figure 2.1 Climate Control Room



Figure 2.2 Interior of Climate Control Room with Coated Specimens and Control Cylinder with Thermocouple

As this study is primarily concerned with the initial concentration of moisture in a bridge pier, the first group of cycles after coating application are naturally the most important. It was decided that 150 freeze-thaw cycles equivalent of almost three years worth of weathering in Ohio were adequate for this study. It is assumed that for a given concrete structure after about 3 years time, either the original moisture has mostly diffused out of the concrete (leaving it sufficiently dry), or that other moisture

has taken its place due primarily to the passage of traffic or precipitation. The latter case is outside the scope of this project.

Table 2.3
Climate Data: Freeze/Thaw Cycles

Location	Season	Number of Cycles
Toledo	1989-1990	50
	1990-1991	51
	1993-1994	62
	1994-1995	58
Dayton	1987-1988	53
	1988-1989	56
	1989-1990	52
	1990-1991	60

The average change in temperature in a freeze/thaw cycle for the years 1989-1990 and 1990-1991, as shown in Table 2.4, gives an idea of the typical range of temperatures in an average cycle. As the capability of the climate control facility was adequate to supply this, conditions comparable to those in the field were assured.

Table 2.4
Climate Data: Average Temperature Change (ΔT) in a Freeze/Thaw Cycle

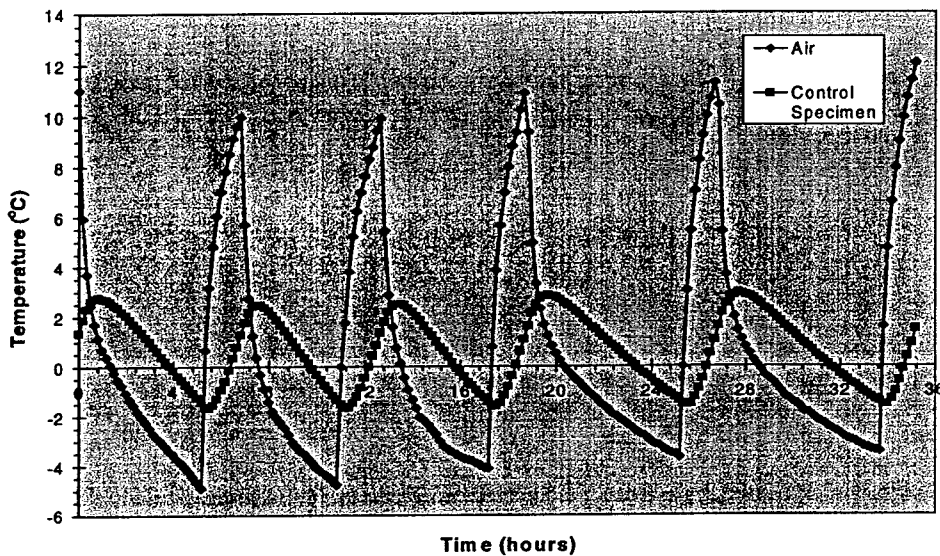
Location	Season	ΔT (in °C)
Toledo	1989-1990	11.6
	1990-1991	12.7
Dayton	1989-1990	13.9
	1990-1991	12.6

The computer program that controlled the temperature of the climate-control room was set to refrigerate the room until the core temperature in the concrete control cylinder reached -1.5°C , and heat the room until the concrete core temperature

reached $+1.5^{\circ}\text{C}$. This results in an average change in air temperature $\Delta T = 15^{\circ}\text{C}$, which is greater than that experienced in the field. Figure 2.3 shows the temperature variation over the course of several typical freeze-thaw cycles. The condition of the coatings was visually monitored during cycling.

Figure 2.3

Typical Freeze/Thaw Cycle Temperature Variation



After completing the 150 freeze/thaw cycles, the specimens were visually and petrographically examined. Twenty-one selected specimens were tested in uniaxial compression following ASTM Standard C 39, "Standard Test Method for Compressive Strength of Cylindrical Concrete Specimens" with a Riehle compression test machine to ascertain the deleterious effects, if any, due to encapsulation. Two coated and weathered 4 x 8 in. concrete cylinders were cut with a Norton Clipper Blockbuster Classic diamond-tipped saw. The same was also done for a control specimen. The resulting 0.75 in. thick cross-sectional slices were polished with a

Struers RotoForce-3 and RotoPol-31 polishing apparatus. Each slice was first ground at 300 RPM for about 20 seconds with an accompanying force of 320 N. The polishing procedure consisted of two steps. The slice was first polished with a lapping disc at 150 RPM at 320 N for 2.5 minutes. The lapping disc was sprayed with a 15 μm diamond spray. During the second step the slice was polished with a polishing disc sprayed with a 9 μm diamond spray. The force, time and revolutions per minute remained the same for the second polishing step.

In addition, forced resonance frequency tests were conducted on eight other specimens in accordance with ASTM Standard C 215, "Standard Test Method for Fundamental Transverse, Longitudinal, and Torsional Frequencies of Concrete Specimens". The transverse frequency was measured with a Geotest C-2010 Sonometer.

2.3 Task 2 - Measurement of Moisture Concentration

This task focused on the measurement of moisture content in uncoated specimens, and the development of a technique for determining the moisture content diffusing through concrete at a specific location. Since weight changes were used to measure diffusion properties, it was assumed that the diffusion rate in the concrete is independent of location, i.e., the sample is homogenous. A Vaisala HMP36 Humidity and Temperature Probe, which uses an operating principle based on changes in the

capacitance of a thin polymer film as it absorbs water molecules, was used to measure the relative humidity in two 6 x 12 in. concrete cylinders.

In order to measure the percent relative humidity within the concrete, three 0.5 in. diameter holes, (enough to accommodate the thickness of the probe), were drilled in a 6 x 12 in. concrete cylinder parallel to its longitudinal axis with radial distances of 2, 1.5 and 0 in. from the center of the cylinder. The depth of the holes was staggered to mitigate the effects of the holes in relation to each other, resulting in holes that were 5.5, 6.0 and 6.5 in. deep.

The holes were closed with rubber plugs between readings so that the moisture in the hole would be representative of the boundary conditions. The specimen was then placed on a screen in a sealed container. Beneath this screen a layer of desiccating material was placed to insure a boundary condition with zero percent relative humidity. When a humidity reading was to be taken, the concrete cylinder was removed from the drying box and the plug from the hole in which the probe was to be placed was removed. Immediately the probe was inserted in the hole and any remaining space at the mouth of the hole was covered to prevent the outside air from interfering with the reading. Electrical tape worked well for this purpose. The probe was left in the hole for 45 minutes before a reading was acquired. This was done to allow the sensor to adjust to the humidity change and stabilize. After the first measurement was recorded subsequent readings were taken at 15 minute intervals. The concrete cylinder was also weighed each time the humidity measurements were performed, so that the two types of data could be compared.

2.4 Task 3 - Freeze/Thaw Durability

For this task two batches of 6 x 12 in. concrete cylinders were cast and cured for 28 days. Since the first batch had lower compressive strength than expected, a second batch was cast.

2.4.1 First concrete batch

The same two curing environments as in Task 1 were used, and a new sealant was added to the project, a water dispersed epoxy (Coating IV). Some of the specimens were partially coated. Selected cylinders were left uncoated at one end, while for others one quadrant of the cylindrical surface was left uncoated. The latter is common practice of O.D.O.T. for bridge piers (Inter-office communication between B.D. Hanhilaammi and D.W. Leake, 1993). Table 2.5 describes the four parameter categories. Also, four uncoated specimens were prepared (three for Curing Environment 1, one for Curing Environment 2).

A total of fifty-two specimens was placed in flexible cylindrical containers filled with water. The containers provided a layer of water approximately 2 mm thick between the container wall and the concrete surface. This was done in accordance with the ASTM Standard Test C 666, "Standard Test Method for Resistance of Concrete to Rapid Freezing and Thawing". The recommendations of this test stipulate that the specimen be surrounded by not less than 1 mm, nor more than 3 mm of water while it is being subjected to freeze/thaw cycling. The specimens were then subjected

to 60 freezing/thawing cycles and examined visually. The surface area of all damaged regions was recorded on tracing paper and calculated with the aid of image analysis software. Selected specimens were tested in uniaxial compression, and others were evaluated by forced resonance frequency tests.

Table 2.5
Parameters for Task 3 Concrete Batch 1

Coating	<ol style="list-style-type: none"> 1. I 2. II 3. III 4. IV 5. Uncoated
Curing Environment	<ol style="list-style-type: none"> 1. Curing Room with 100% RH 2. Specimens covered with wet burlap and plastic
Coating Application	<ol style="list-style-type: none"> 1. Fully Coated 2. Fully Coated except for one end 3. Fully Coated except for one quarter of cylindrical surface
Number of Specimens	<ol style="list-style-type: none"> 1. Three for each combination of parameters that included Curing Environment 1 ($4 \times 3 \times 3 + 3 = 39$). 2. One for each combination of parameters that included Curing Environment 2 ($4 \times 3 \times 1 + 1 = 13$).

2.4.2 Second concrete batch

A total of forty-three (43) specimens were placed in newly constructed sheet metal cylindrical containers filled with water. The containers provided a layer of water approximately 2 mm thick between the container wall and the concrete surface. This

was done in accordance with the ASTM Standard Test C 666, "Standard Test Method for Resistance of Concrete to Rapid Freezing and Thawing". The recommendations of this test stipulate that the specimen be surrounded by not less than 1 mm, nor more than 3 mm of water while it is being subjected to freeze/thaw cycling. The specimens were subjected to 250 freezing/thawing cycles and examined visually.

The same two curing environments and the same four sealants as for the first batch were used. For selected cylinders one quadrant of the cylindrical surface was left uncoated. Table 2.6 summarizes the parameter categories considered. Selected specimens were tested in uniaxial compression, and others were evaluated by forced resonance frequency tests.

Table 2.6
Parameters for Task 3 Concrete Batch 1

Coating Type	<ol style="list-style-type: none"> 1. I 2. II 3. III 4. IV 5. Uncoated
Curing Environment	Curing Room with 100% RH (for 28 days) <ol style="list-style-type: none"> 1. Coated 2 days after curing and tested 10 months after coated 2. Coated 10 days after curing and tested 10 months after coated 3. Coated 10 months after curing and tested immediately
Coating Application	<ol style="list-style-type: none"> 1. Fully Coated 2. Fully Coated except for 1/4 of the surface

2.5 Task 4 - Computer Modeling of Diffusion

A Finite Element Method computer program was used to model the diffusion behavior of moisture in a typical specimen. Three-node linear displacement triangular elements were used to model the diffusion of the moisture. In order to determine the initial concentration of moisture within a typical concrete specimen, two specimens from the 100% RH curing room were selected at random and promptly weighed. They had been cured for eight weeks, thus insuring that they were saturated. They were placed in an oven and heated at 500°F for 18 hours, allowed to cool, and weighed again. Based on the difference in mass divided by the volume a value for the initial moisture concentration was determined for the computer program used. The program was run iteratively to produce a curve that best fit the experimental data points using the least-squares method (Scheaffer and McClave, 1986). An apparent diffusion coefficient for the concrete used to cast the second batch of specimens was thus determined.

The input file for the computer program was modified to reflect a specimen with a particular coating. The thickness of the coating was measured from a polished cross-sectional slice of a specimen using a microscope and imaging software. Based on twenty thickness measurements along the perimeter of the concrete slice, an average value for a typical thickness for the coating in question was obtained. This was done for the Coatings II, III and IV. For Coating I, no discernible coating thickness could be observed even with the aid of the microscope. However, the depth

to which it penetrated was determined by applying a thin film of water to the surface of the slice and then measuring through the microscope the average depth over which the water was repelled. The computer program was then run in a similar manner to determine the apparent diffusion coefficients of each coating or the layer of the specimen that the coating penetrated into. These predicted values for each coating were compared to experimental findings based on percent mass loss averaged for two specimens allowed to dry in air.

CHAPTER THREE

DISCUSSION OF RESULTS

3.1 Task 1 - Investigation of Moisture Encapsulation

After 150 freeze-thaw cycles in the climate control room, no damage was observed on the surface of the specimens to the concrete or the coating. Even the coating/substrate interface indicated no degradation. To obtain more quantitative information, compression tests were performed on sealed samples.

The compressive strength values for the weathered specimens are shown in Table 3.1. The compressive strengths are categorized according to overall performance of each coating and according to the varying parameters in Figures 3.1 and 3.2, respectively. It can be readily seen that all of the “weathered” specimens exhibited a higher compressive strength than those that had been excluded from the experiment. However, the compressive strength of the specimens seems at least marginally linked to the permeability of the coating. The specimens sealed with the most permeable coating (Coating I) exhibited the highest compressive strength, while those with the least permeable coating (Coating II) had the least strength. Nevertheless, even the specimens that were sealed with the latter showed an *increase* in strength of 1.8% when compared to specimens that had remained in the curing room for about 4 months. This was probably due to the continuation of the hydration process, as moisture retained by the coating which otherwise would have been lost aided curing. This seems to indicate that moisture encapsulation is not a significant

factor contributing to degradation of concrete in the field, though it may play some minor role as far as compressive strength is concerned.

Table 3.1
Compressive Strength Test Results on 6 x 12 in. (15.2 x 30.5 cm)
Cylinders From Task 1 (1,000 psi = 6.9 MPa)

Coating Type	Curing Duration	Air Drying	Curing Environment	Compressive Stress (psi)
Uncoated*	28 days	0 days	100% RH	6,578
				6,225
				6,667
Uncoated*	4 months	0 days	100% RH	6,932
				6,693
				6,543
I II III	7 days	0 days	100% RH	7,427
				6,225
				7,551
I II III	28 days	0 days	100% RH	7,471
				6,278
				7,321
I II III	28 days	0 days	"Field conditions"	8,037
				6,357
				7,418
I II III	28 days	30 days	100% RH	7,286
				7,958
				7,967
I II III	28 days	30 days	"Field conditions"	8,064
				7,392
				7,498

Notes:

* No freeze/thaw exposure

This view is further bolstered by examination of Figure 3.2, which does show that the specimens with the lowest strength were sealed in accordance with parameters that guaranteed more moisture in the concrete at the onset of freezing, regardless of what coating was used. Therefore, specimens coated immediately after the allotted

curing time were weaker than those allowed to dry for 30 days after curing before sealant application (about 93% of the air dried specimens). The captions describe the duration of curing, the relative humidity during curing, and the days air dried for each group, respectively.

Figure 3.1

**Average Compressive Strength Test Results
Depicting Overall Coating Performance**

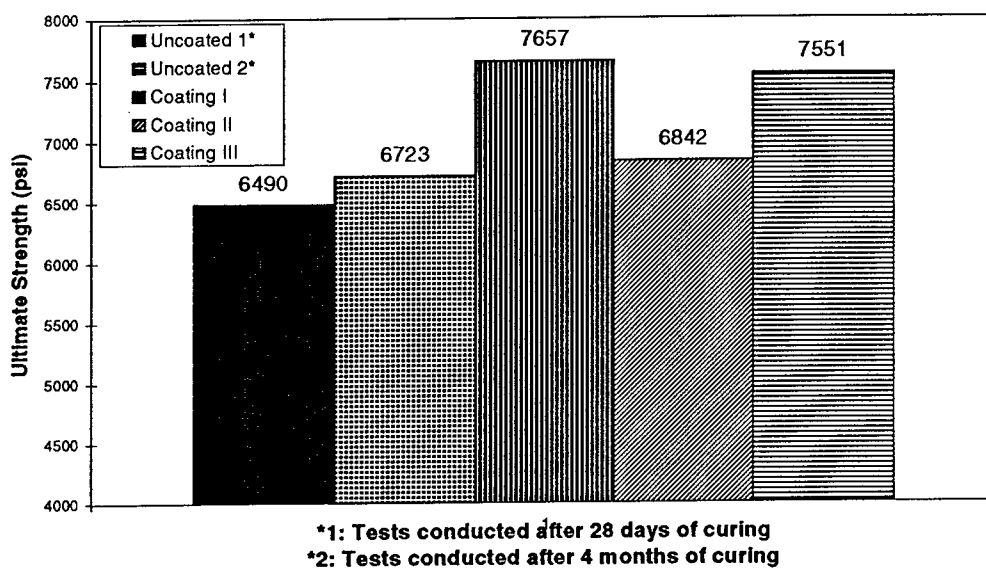
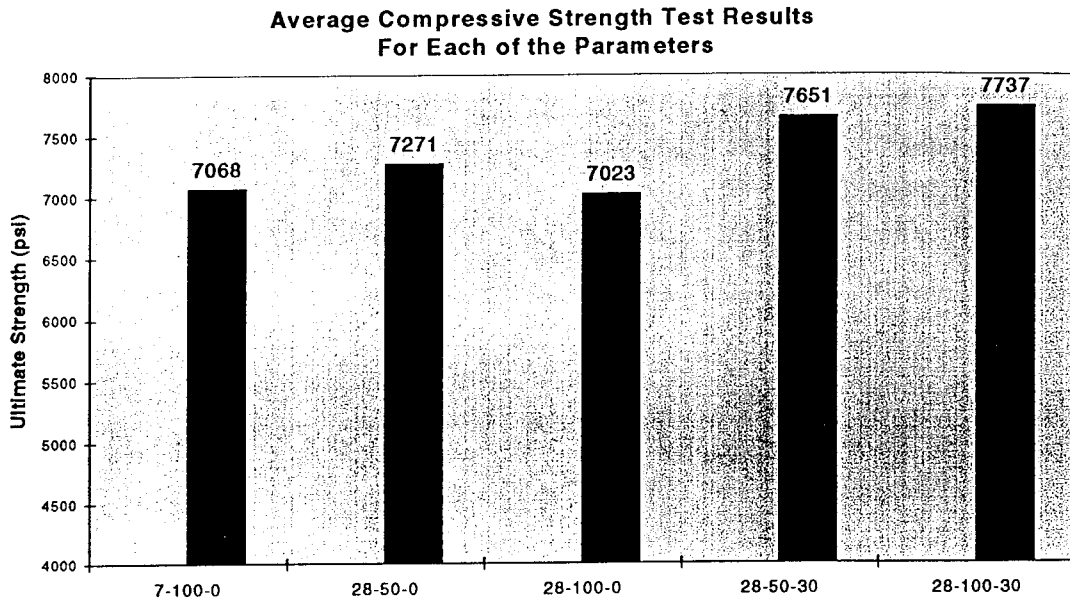


Figure 3.2



The lack of surface deterioration apparent to the naked eye did not necessarily mean that no damage had occurred. For example, laboratory concrete subjected to 300 cycles in an experiment conducted by Bakharev and Struble [1995] displayed no visible cracking until microscopical examination revealed "...vertical cracks extending from the surface to a depth of 200 mm or more, and spaced 10 to 15 mm apart." In order to inspect the specimens further, a slice was cut from two 4 x 8 in. cylinders cured for 28 days at 100% RH that were coated with the two most impermeable coatings immediately subsequent to the conclusion of curing (i.e., the "worst case scenario"). The slices were polished and examined with a microscope, and compared with a slice cut from an uncoated cylinder which had not been subjected to freeze-thaw cycling. Any cracks observed would be indicative of degradation, thus

substantiating the claim that moisture encapsulation is a problem. No cracks or fissures of any kind were found in the weathered specimen. Figure 3.3 depicts a portion of the cross section of the “weathered” specimen coated with Coating II, and Figure 3.4 shows a cross sectional view of the unweathered one.

Measurement of the resonant frequency is another method intended to detect deterioration in concrete. The dynamic modulus of elasticity, E_d , calculated from the results of the resonant frequency test, is reported for the 6 x 12 in. concrete cylinders in Table 3.2. Again, it seems that no damage occurred, as the average dynamic modulus for the two unweathered concrete cylinders was found to be 4.60×10^6 psi, while the average E_d for the “weathered” specimens was 4.69×10^6 psi.

Table 3.2
Resonance Frequency Test Results from Task 1

Coating Type	Curing Duration	Air Drying	Curing Environment	E_d (psi)
uncoated	28 days	5 months	100% RH	4.55×10^6
uncoated		5 months		4.66×10^6
I		5 days		4.43×10^6
II			4.96×10^6	
III			4.64×10^6	
I		“Field conditions”	4.52×10^6	
II	4.83×10^6			
III	4.75×10^6			

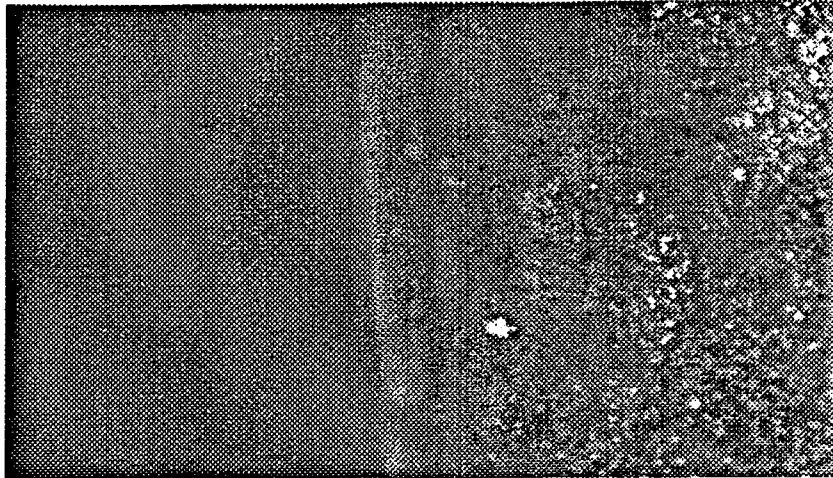


Figure 3.3
Cross-Section of Specimen Coated with Coating 2
After 150 Freeze/Thaw Cycles (field of view 1240x 920 microns)



Figure 3.4
Uncoated Specimen not Subject to Freeze/Thaw
Cycling (field of view: 1240x920 microns)

3.2 Task 2 - Measurement of Moisture Concentration

The relative humidity (RH) measurements were qualitatively predictable. The measurements in the center hole of the cylinder always yielded the highest reading. The further away from the center of the cylinder, the lower was the RH. For the first several days the readings remained at a maximum, reflecting the saturated condition of the specimen. At this point the water content of the concrete was higher than the concentration of saturated air at room temperature, but eventually a pattern developed. The curves of % RH versus time are plotted in Figure 3.6. The percent mass loss is plotted as a function of time for the same specimen in Figure 3.5. Since the initial moisture concentration for the concrete used was determined during the course of Task 4, the percent mass loss measurements could be used to obtain the concentration at any time.

What is required is a relationship between the % RH readings and the moisture concentration. Let's assume that the % RH readings are plotted versus the radial distance from the longitudinal axis of the concrete cylinder, x , and a polynomial curve fit for the data of the form

$$y = a_0 + a_1x^2 + a_2x^4 + a_3x^6 \quad (3.1)$$

is used. The "moisture profile" based on the above curve fit at a given time is shown in Figure 3.7. Note that the % RH for the specimen surface is assumed to be zero for a time $t > 0$, since the water at the surface is the first to diffuse into the ambient air.

If the “moisture profile” curve is revolved around the vertical axis so that a solid is swept out, then its volume will be proportional to the concentration. The generated volume of revolution is

$$V = \int_a^b 2\pi x f(x) dx \quad (3.2)$$

where $a = 0$ in. and $b = +3$ in. ($a \leq x \leq b$).

Finally, the volumes can be plotted versus their corresponding concentrations. The initial and final conditions provide the endpoints of the curve. The 100% RH, which reflects the initial saturated condition of the concrete, results in a cylindrical volume of

$$V = \pi r^2 h = \pi(3)^2 100 = 2827.4 \text{ cm}^2 \%RH \quad (3.3)$$

Similarly, at $t = \infty$ the %RH will be zero everywhere, giving a volume of zero. The volume, V , plotted as a function of C , the concentration, is practically linear with the equation of the straight line fit being $\%RH = 14,928C$ with a correlation coefficient of 0.999 (see Figure 3.8).

This relationship is useful for field work because the concentration can now be easily obtained for a set of %RH measurements, i.e. the specimen need not be weighed. This is fortunate as it is rather difficult to “weigh” a bridge pier.

Figure 3.5

Percent Mass Loss of Drying 6 x 12 In. Concrete Cylinder In Humidity Experiment

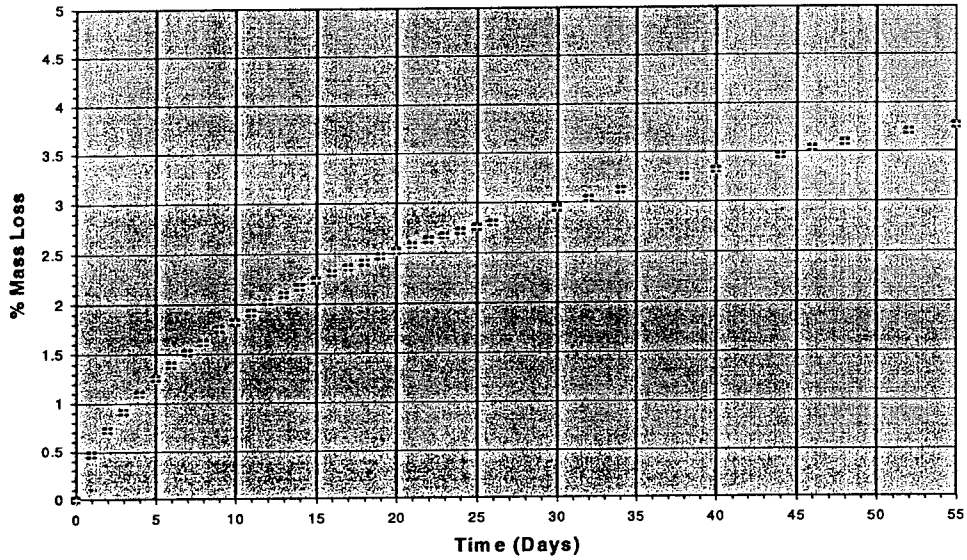


Figure 3.6

Humidity Measurements in a 6 x 12 in. Concrete Cylinder at Radial Distances of 0, 1.5 and 2 in.

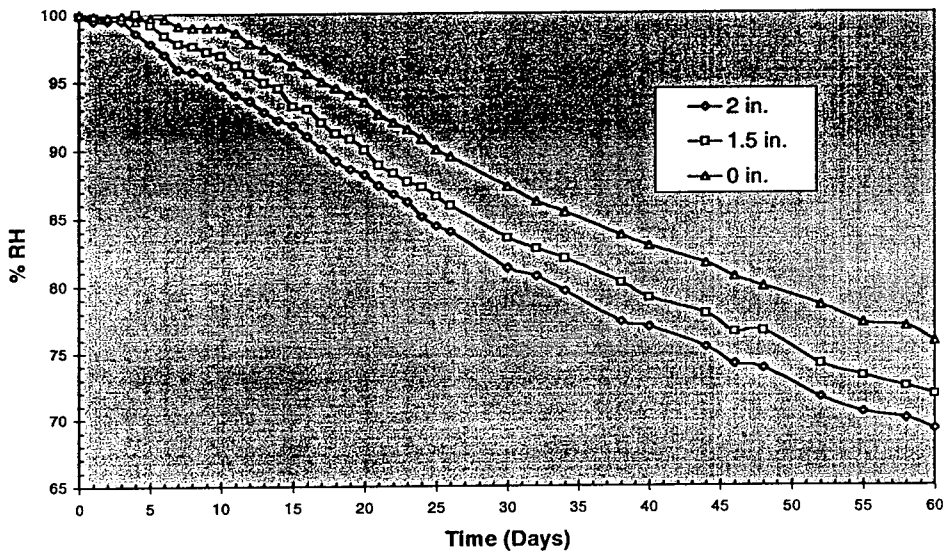


Figure 3.7

Distribution of Moisture within Specimen

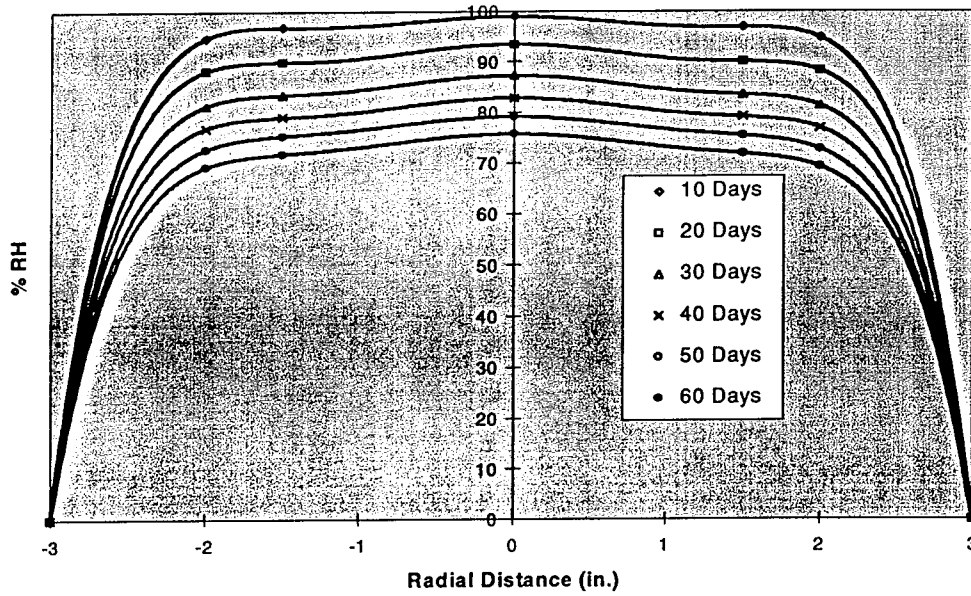
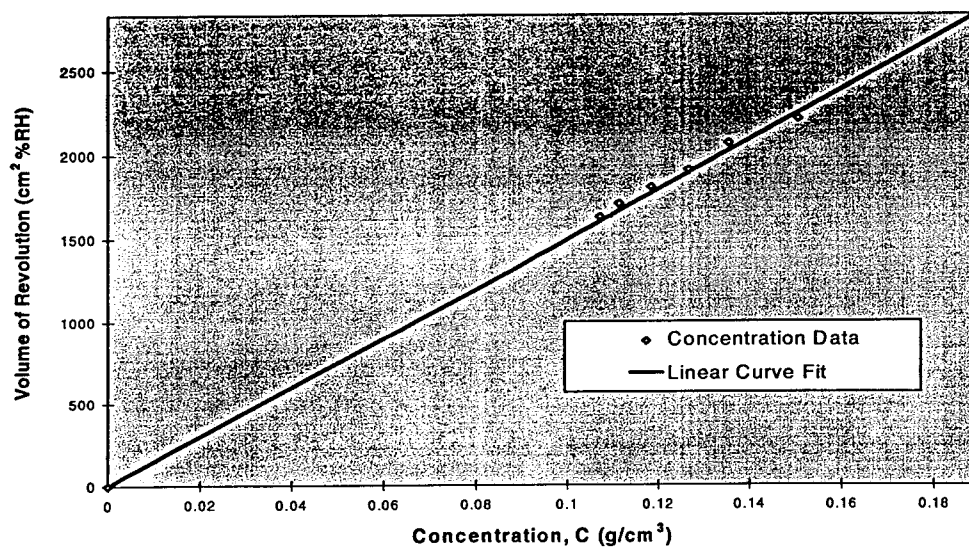


Figure 3.8

Volume/Concentration Curve for 6 x 12 in. (15.2 x 30.48 cm) Specimen



3.3 Task 3 - Freeze/Thaw Durability

3.3.1 First Concrete Batch

After the 60 freeze/thaw cycles were complete, the specimens as a whole were found to have sustained noticeable damage. Concrete had spalled and cracked in many places. There was also considerable flaking and peeling of the epoxy coatings. Figures 3.9 - 3.25 show the specimens after the completion of the freeze/thaw cycling, with the damaged regions outlined with a black marker for specimens treated with coatings not readily noticeable. The damaged areas of each concrete cylinder as a percentage of the total surface area is shown in Table 3.3. In addition, the number of damaged regions as well as the average area for each region for each specimen are reported in Table 3.3.

The specimen identification characters are as follows: a cylinder completely coated was assigned a "1", one left uncoated on the top a "0", and a specimen left uncoated on a quadrant of the cylindrical surface "1/4". As mentioned previously, a Roman numeral designates each coating type. A "U" means the specimen was uncoated, and an "A", "B" or "C" distinguishes specimens within a group of the same parameter category.

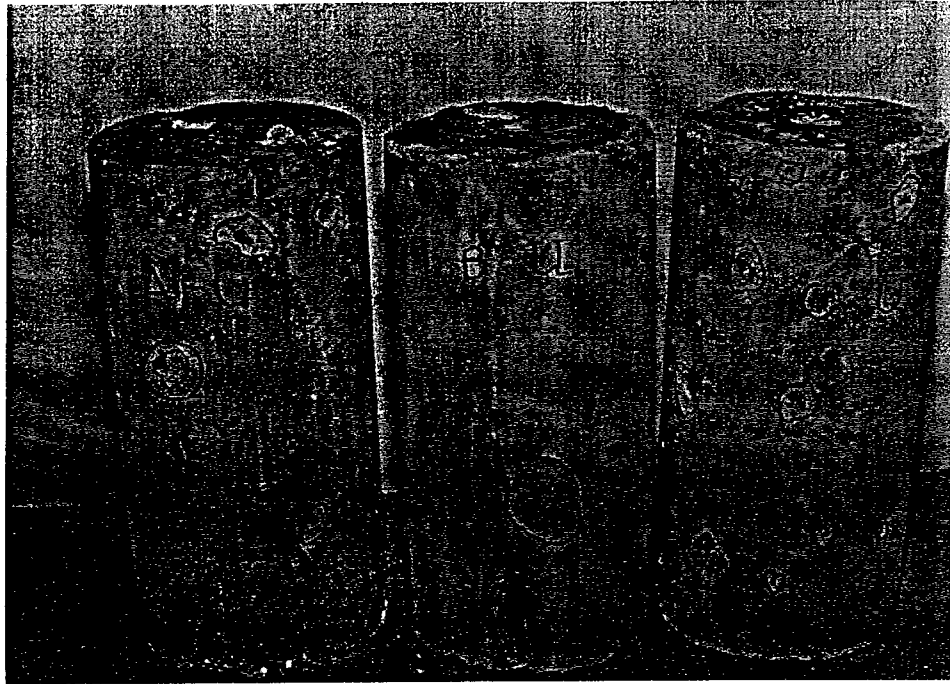


Figure 3.9 - Uncoated Specimens (A-U, B-U and C-U)

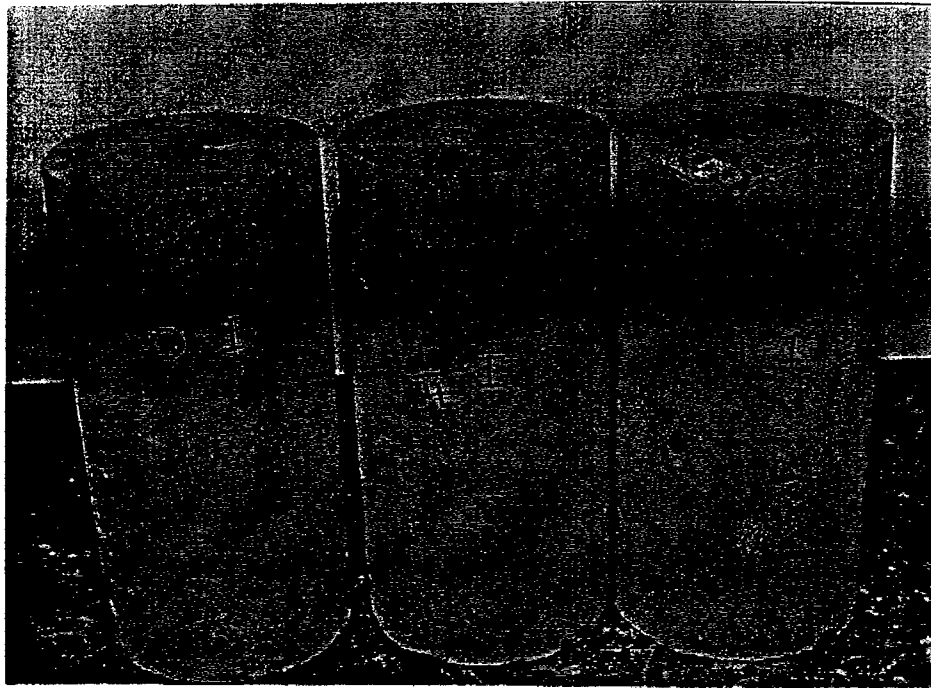


Figure 3.10 - Specimens Cured Outside and Coated with Coating I (0-I, 1/4-I and 1-I)

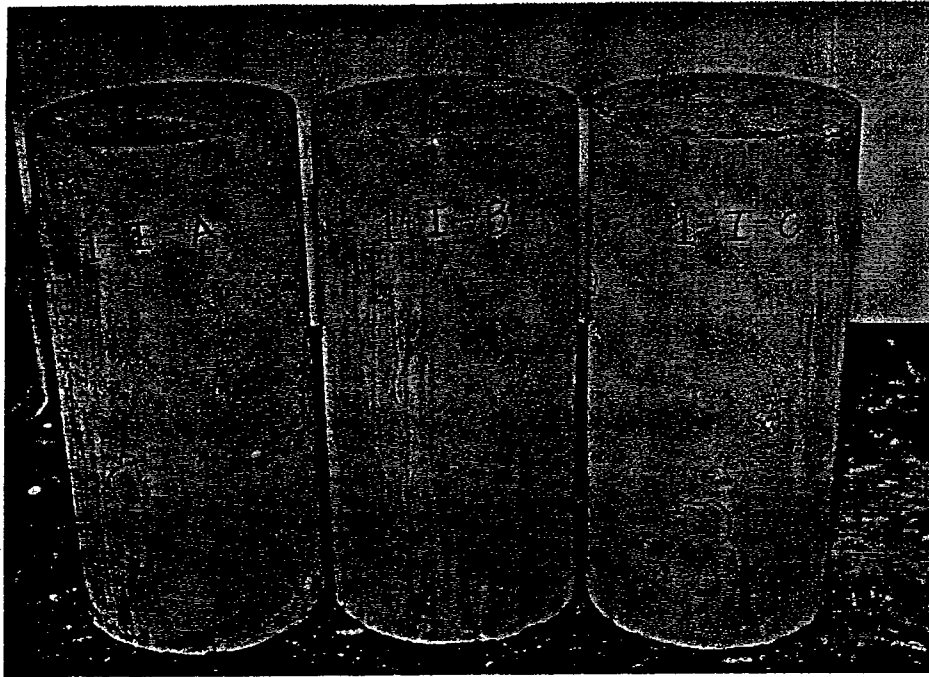


Figure 3.11 - Specimens Cured Inside and Coated with Coating I (1-I-A, 1-I-B and 1-I-C)

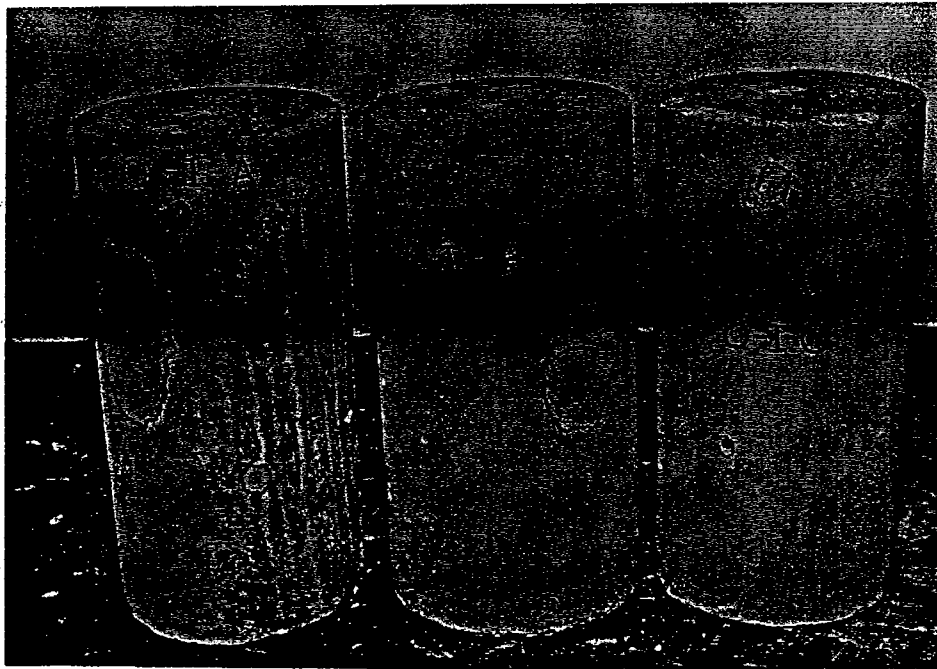


Figure 3.12 - Specimens Cured Inside and Coated with Coating I (0-I-A, 0-I-B and 0-I-C)

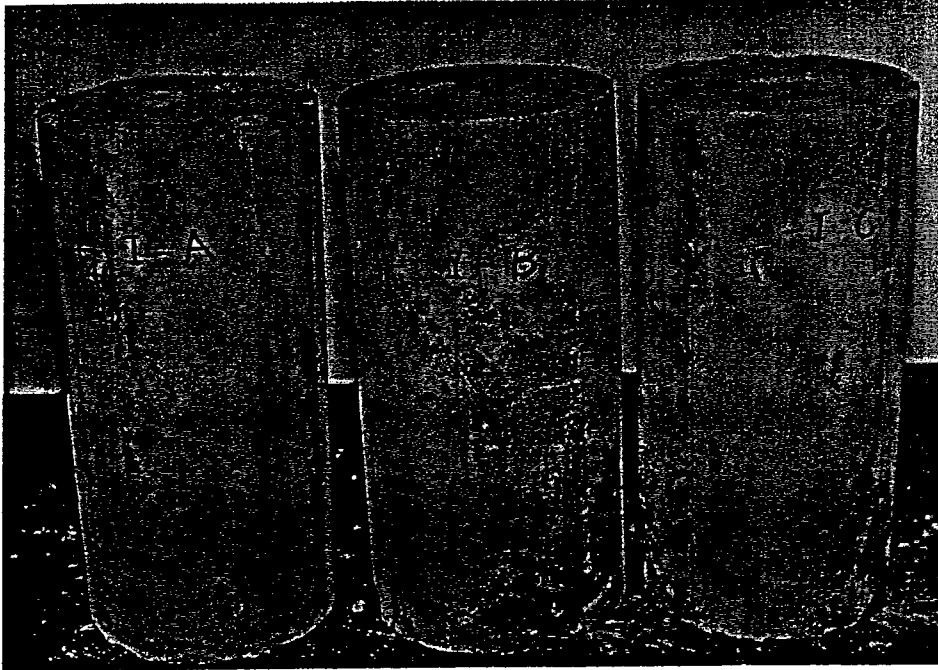


Figure 3.13 - Specimens Cured Inside and Coated with Coating I (1/4-I-A, 1/4-I-B and 1/4-I-C)

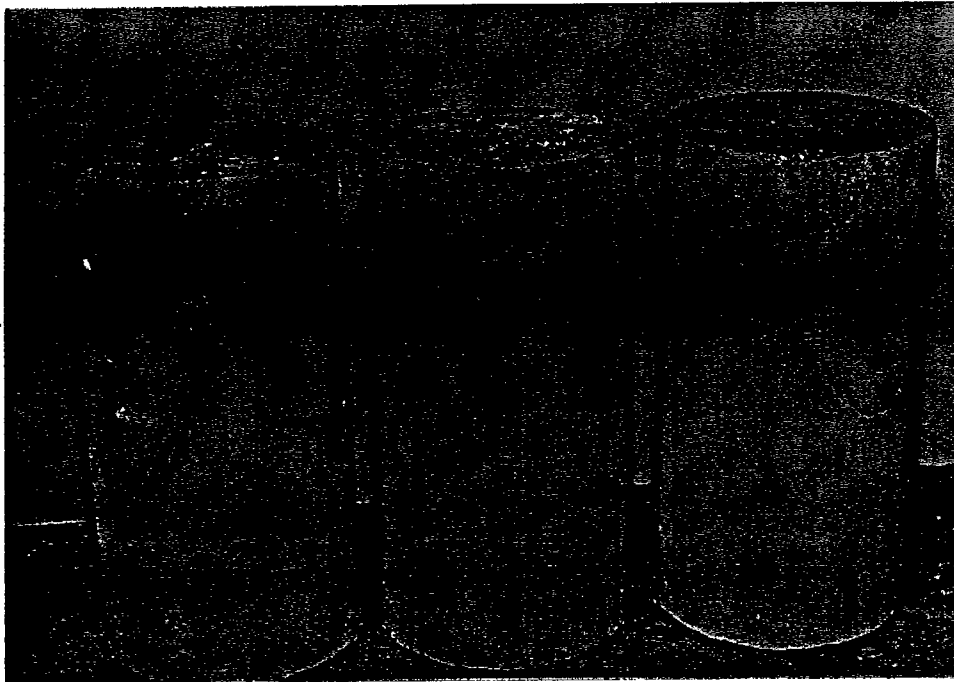


Figure 3.14 - Specimens Cured Outside and Coated with Coating II (1-II, 1/4-II and 0-II)

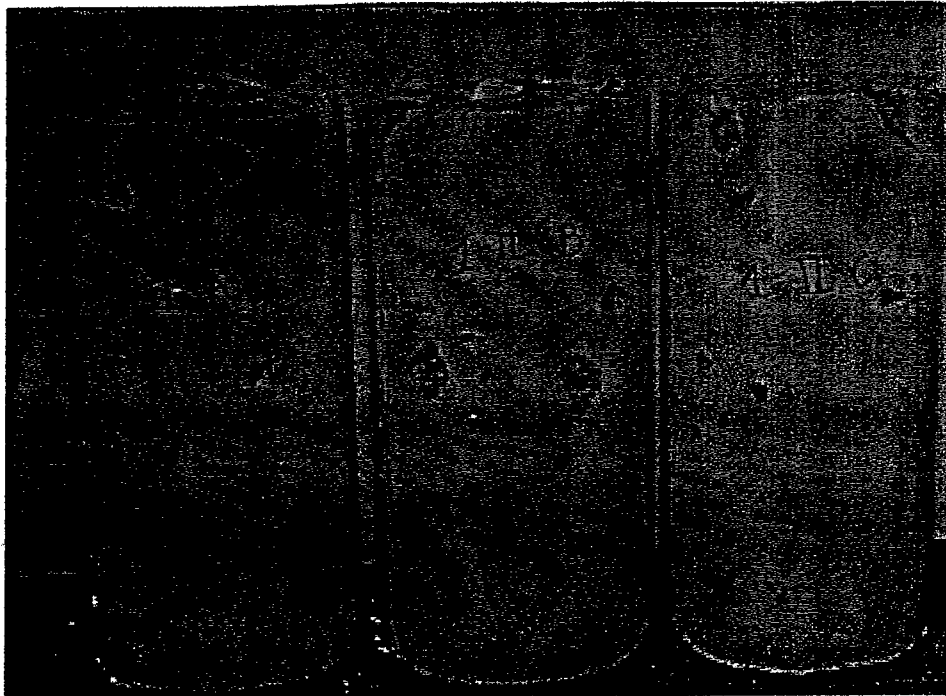


Figure 3.15 - Specimens Cured Inside and Coated with Coating II (1-II-A, 1-II-B and 1-II-C)

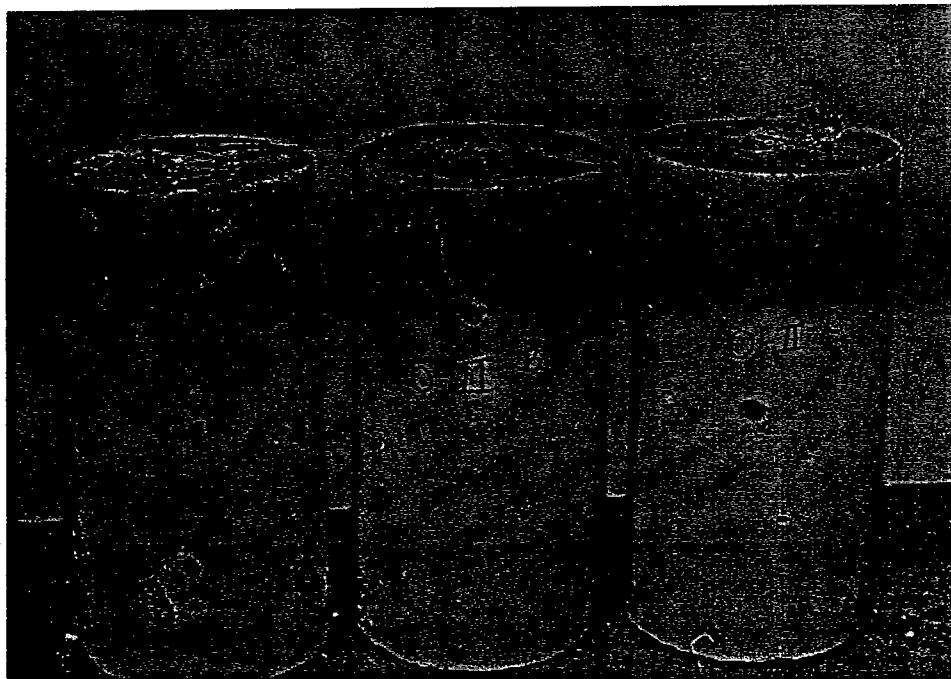


Figure 3.16 - Specimens Cured Inside and Coated with Coating II (0-II-A, 0-II-B and 0-II-C)

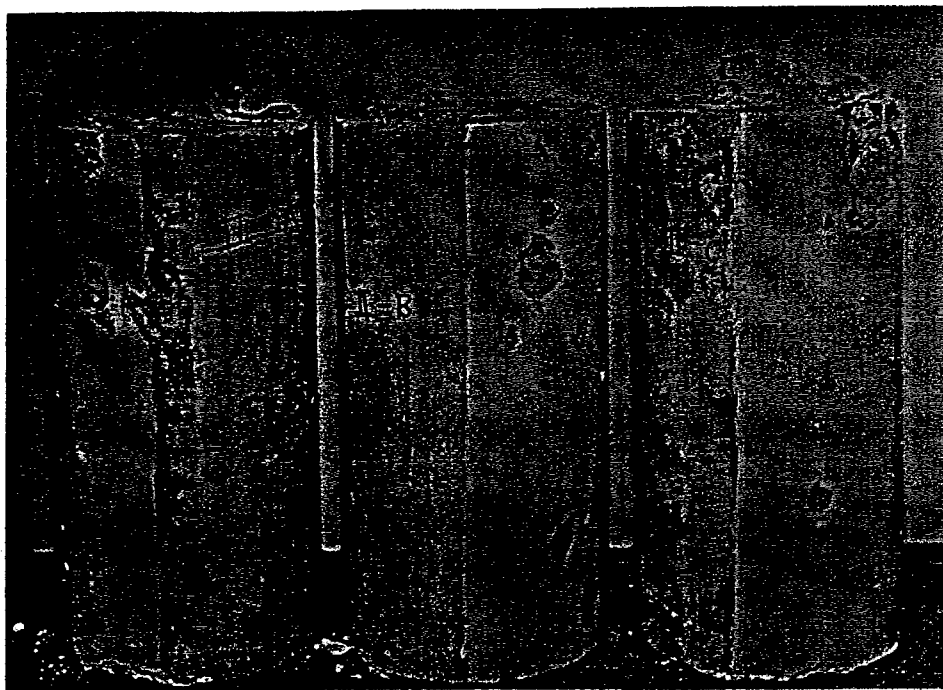


Figure 3.17 - Specimens Cured Inside and Coated with Coating II (1/4-II-A, 1/4-II-B and 1/4-II-C)

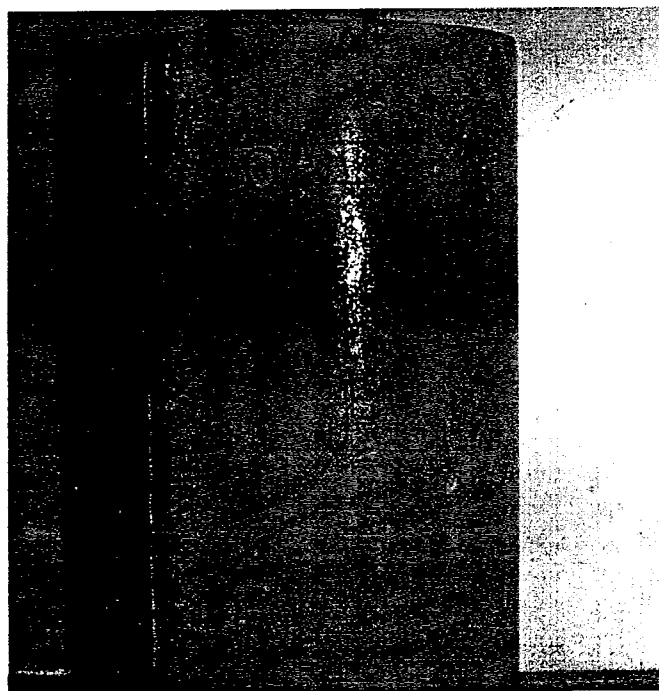


Figure 3.18 - Specimen Cured Outside and Coated with Coating III (0-III)

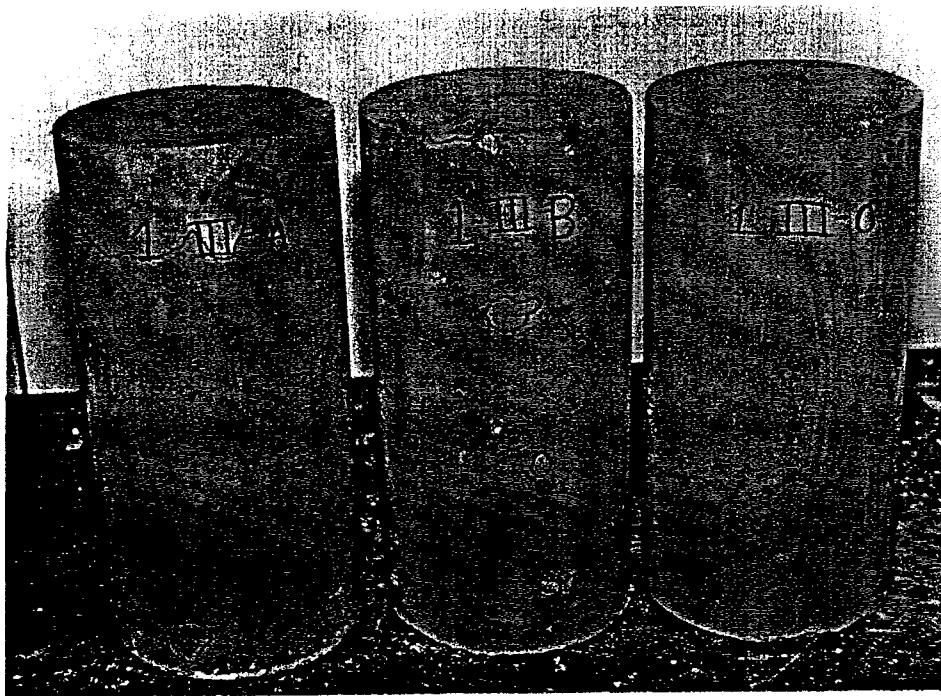


Figure 3.19 - Specimens Cured Inside and Coated with Coating III (1-III-A, 1-III-B and 1-III-C)

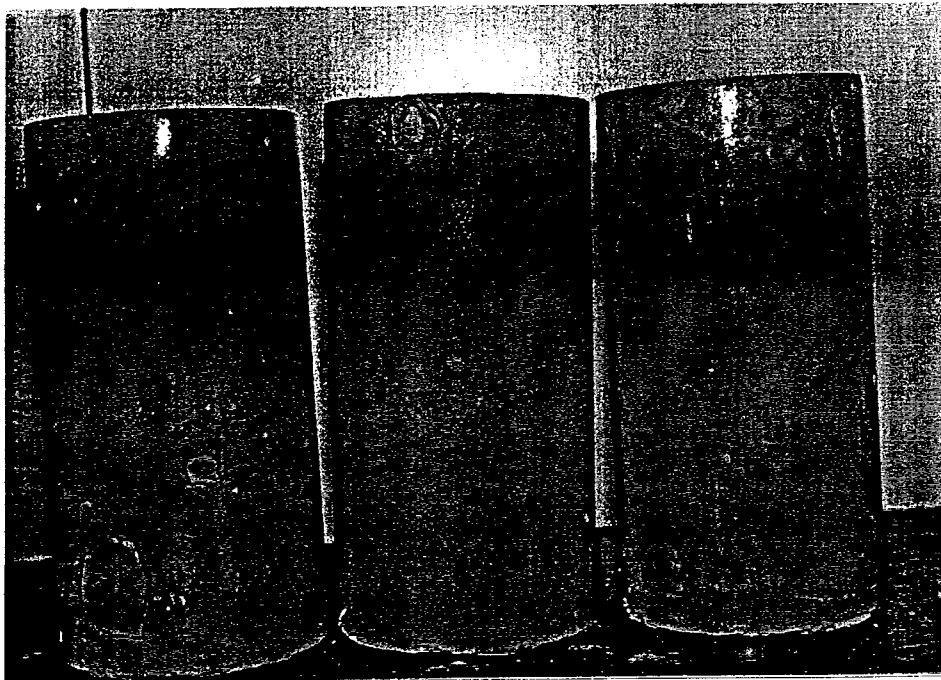


Figure 3.20 - Specimens Cured Inside and Coated with Coating III (0-III-A, 0-III-B and 0-III-C)

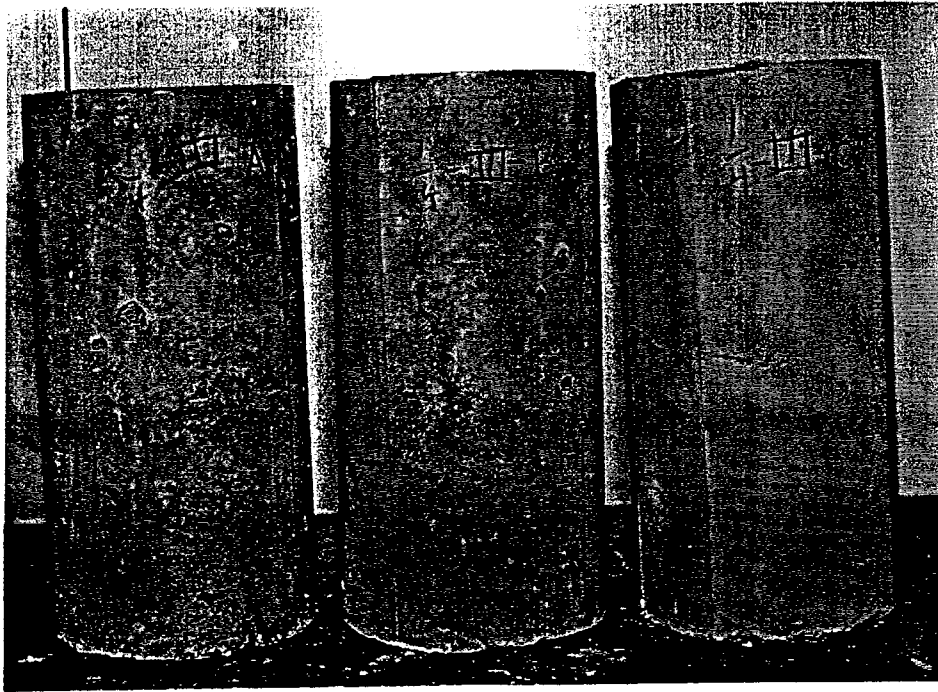


Figure 3.21 - Specimens Cured Inside and Coated with Coating III (1/4-III-A, 1/4-III-B and 1/4-III-C)

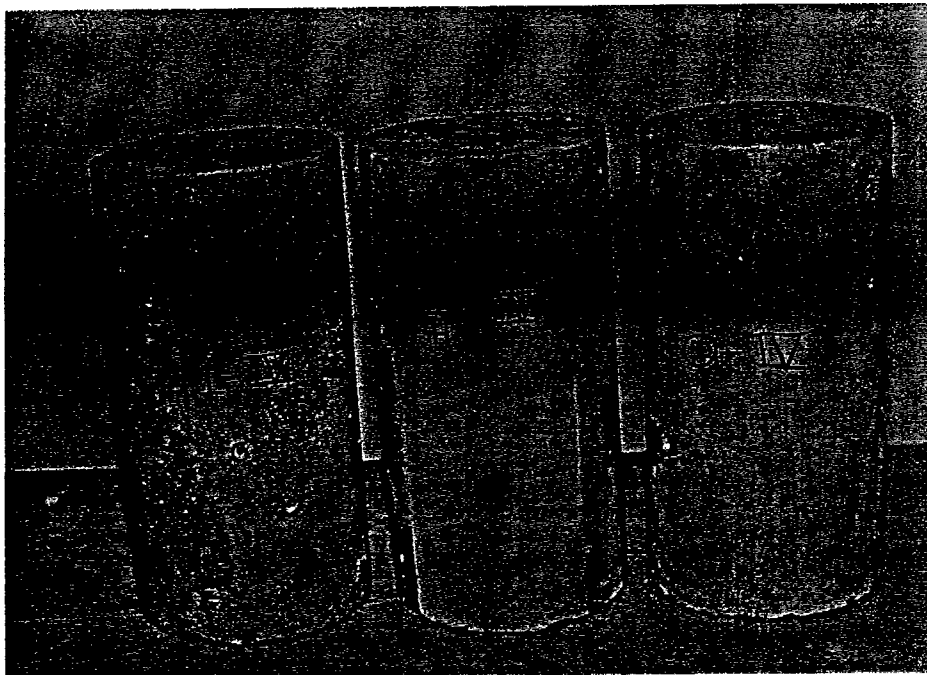


Figure 3.22 - Specimens Cured Outside and Coated with Coating IV (1-IV, 1/4-IV and 0-IV)

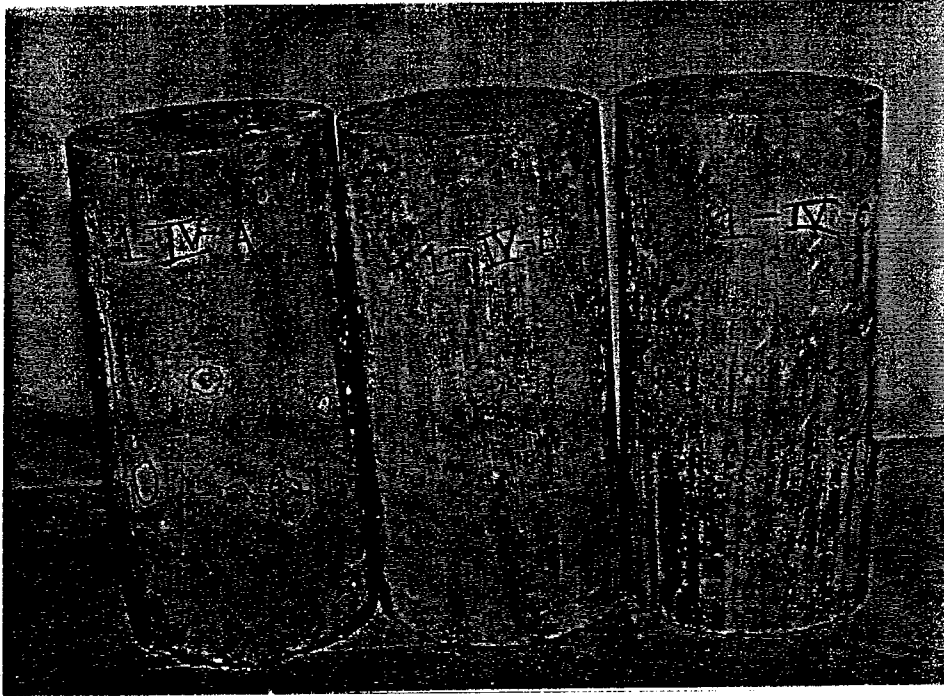


Figure 3.23 - Specimens Cured Inside and Coated with Coating IV (1-IV-A, 1-IV-B and 1-IV-C)

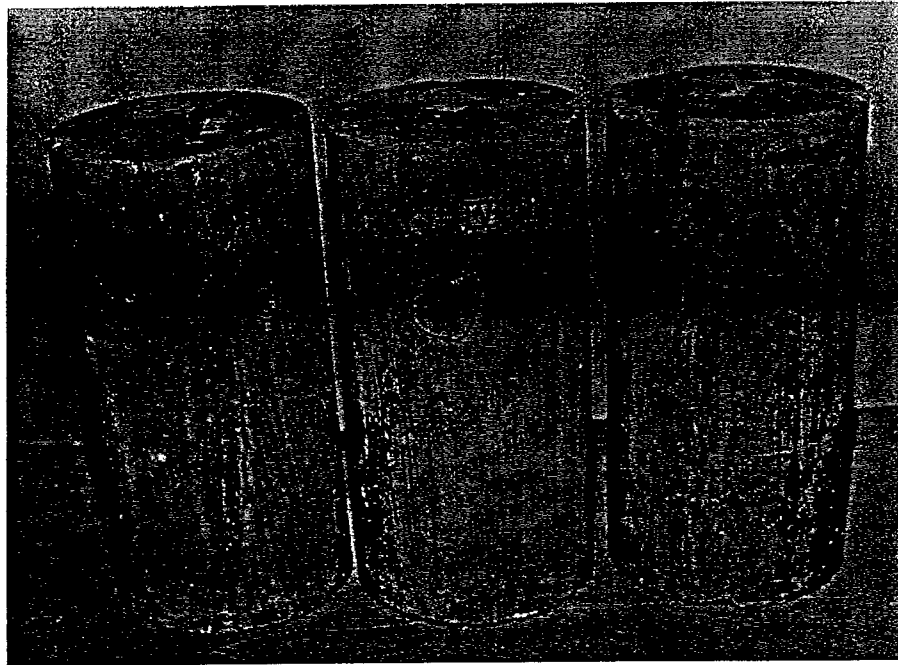


Figure 3.24 - Specimens Cured Inside and Coated with Coating IV (0-IV-A, 0-IV-B and 0-IV-C)

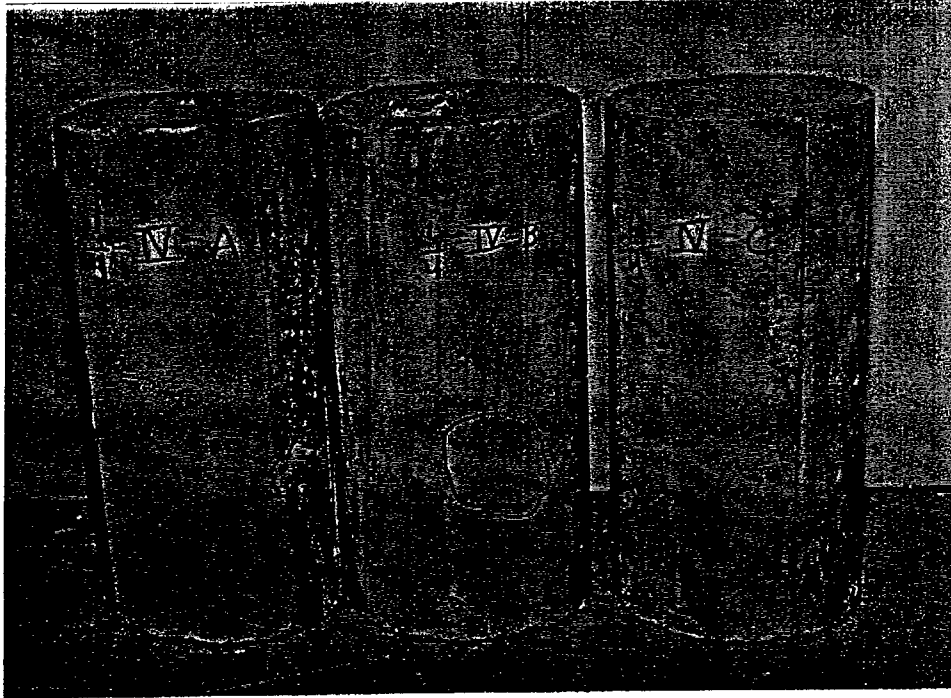


Figure 3.25 - Specimens Cured Inside and Coated with Coating IV (1/4-IV-A, 1/4-IV-B and 1/4-IV-C)

Table 3.3
Damage Data for Task 3

Specimen	Damaged Regions as % of Total Surface Area	Number of Damaged Regions	Average Area of Damaged Regions (cm²)
1-I-A	1.6	5	5.2
1-I-B	0.2	1	3.1
1-I-C	1.9	7	4.3
1-I	1.1	2	9.2
1/4-I-A	0.4	2	2.9
1/4-I-B	0.1	1	1.7
1/4-I-C	2.1	5	6.8
1/4-I	0.2	1	3.0
0-I-A	3.7	8	7.6
0-I-B	2.4	9	4.3
0-I-C	0.9	6	2.5
0-I	0.0	-	-
1-II-A	3.9	19	3.4
1-II-B	7.0	30	3.8
1-II-C	7.0	26	4.4
1-II	0.4	5	1.4
1/4-II-A	10.0	39	4.2
1/4-II-B	4.4	28	2.6
1/4-II-C	7.1	23	5.0
1/4-II	0.4	6	1.0
0-II-A	6.2	25	4.1
0-II-B	3.2	7	7.5
0-II-C	2.5	12	3.4
0-II	0.1	1	2.2

Table 3.3
Damage Data for Task 3 (Continued)

Specimen	Damaged Regions as % of Total Surface Area	Number of Damaged Regions	Average Area of Damaged Regions (cm²)
1-III-A	6.3	3	35.2
1-III-B	1.1	8	2.3
1-III-C	0.0	-	-
1-III	0.0	-	-
1/4-III-A	0.7	1	11.6
1/4-III-B	0.0	-	-
1/4-III-C	0.7	5	2.3
1/4-III	0.1	1	1.8
0-III-A	3.4	6	9.4
0-III-B	3.6	4	14.7
0-III-C	0.1	1	2.2
0-III	0.0	-	-
1-IV-A	1.1	6	3.1
1-IV-B	0.2	2	1.8
1-IV-C	0.0	-	-
1-IV	0.0	-	-
1/4-IV-A	0.6	2	5.2
1/4-IV-B	2.0	2	16.1
1/4-IV-C	0.0	-	-
1/4-IV	0.0	-	-
0-IV-A	2.3	4	9.6
0-IV-B	1.8	1	29.1
0-IV-C	0.0	-	-
0-IV	0.0	-	-
U-A	2.0	5	6.5
U-B	2.7	6	7.3
U-C	2.9	20	2.4
U-D	0.0	-	-

Table 3.4 summarizes the data in a more meaningful way. Coatings I, III and IV showed some effectiveness in protecting the concrete surface, as the surface area that spalled for these coatings was on the average smaller than the damaged surface area for uncoated concrete specimens. Coating II is a notable exception to this, though whether this is due to its considerable impermeability, or to some other factor is not known. Judging from the results, it matters little how much of the surface area is coated.

Table 3.4
Average Spalled Concrete Area as % of Total
Surface Area for Different Parameter Categories

Coating Type	
I	1.2
II	5.0
III	1.8
IV	0.7
U	1.9
Coated Surface Area	
1	2.0
1/4	1.8
0	1.9
Specimens Cured in 100% RH	
2.4	
Specimens Cured at "Field Conditions"	
0.2	

Tables 3.5 and 3.6 report and summarize the compressive strengths for selected specimens. Again, it can be seen that no benefits are gained by leaving areas of the specimens uncoated. As expected, specimens cured at 100% RH (Curing Environment 1) consistently displayed higher strengths, reflecting the benefits of

plentiful water for the hydration process. The other curing environment, however, resulted in the successive wetting and drying of the concrete cylinders, as they were sprayed down once a day and then covered. Therefore, it was inevitable that some drying occurred resulting in higher permeability in the paste (Mindess and Young, 1981). This could be because shrinkage during drying altered the pore-size distribution, permitting capillary pores to become partially interconnected. Such shrinkage will also undoubtedly cause cracking at the aggregate-paste interface, creating more opportunities for the intrusion of water. This would make the concrete more susceptible to frost damage, thereby lowering its compressive strength. On the other hand, critical saturation is harder to reach in the surface concrete of specimens cured in an environment that allows repeated partial drying, because in order for water to enter the concrete, air must leave. Once the original moisture is allowed to escape and is replaced by air in some of the voids, it is difficult to saturate concrete to the point that it achieves its initial unit weight. Thus, when freezing occurs the water has an outlet that would be inaccessible to it otherwise. In other words, the hydraulic pressure that accompanies freezing is sufficient to force some of the water into the otherwise air-filled voids thereby alleviating some of the tension caused by the expansion of liquid moisture as it turns to ice. In addition, the water has the opportunity to take the paths created by the drying into the interior of the specimen, again diverting water before it can give rise to destructive tensile stresses. These are probably the reasons why specimens cured in the curing room exhibited damage that

was more severe at the surface than those that were cured under damp burlap and covered with plastic sheets.

Table 3.5
Compressive Strength of Selected Concrete Cylinders

Specimen	Compressive Strength (psi)
Unweathered	3,944
Unweathered	3,882
Unweathered	3,944
1-I-B	3,890
1-I	4,067
1/4-I-B	4,616
1/4-I	4,094
0-I-B	4,315
0-I	4,085
1-II-A	4,182
1-II	4,333
1/4-II-B	3,537
1/4-II	4,129
0-II-A	4,439
0-II	3,625
1-III-C	4,120
1-III	4,085
1/4-III-B	4,350
1/4-III	3,254
0-III-C	4,147
0-III	4,120
1-IV-A	4,173
1-IV	4,200
1/4-IV-C	4,209
1/4-IV	3,572
0-IV-C	3,554
0-IV	3,422
A-U	3,608
B-U	4,209
C-U	3,979

Table 3.6
Overall Compressive Strength Data for Each Parameter Category

Specimen Characteristic	Average Compressive Strength (psi)	Standard Deviation (psi)
Unweathered	3,923	35
I	4,178	253
II	4,041	373
III	4,013	383
IV	3,855	375
U	3,932	303
Curing Room	4,120	325
"Field conditions"	3,916	349
1	4,131	128
1/4	3,970	466
0	3,963	378

Results from resonant frequency tests conducted on nine weathered specimens and two uncoated, unweathered specimens further indicate that while the weathered specimens did experience degradation as a result of freeze/thaw cycling, coating them did provide some measure of protection. The average dynamic modulus of elasticity for the unweathered specimens was 4.43×10^6 psi, while for coated specimens the average dynamic modulus, E_d , was 4.04×10^6 psi. However, an uncoated specimen exposed to freeze/thaw had a E_d of only 2.48×10^6 psi. It is interesting to note that specimens sealed with coating I exhibited the lowest dynamic modulus, but the highest overall compressive strength. ASTM C 215 cautions, however, that test results "...should not be considered an index of compressive or flexural strength...".

Table 3.7
Dynamic Modulus, E_d , of Selected Concrete Cylinders for the First Batch of Concrete

Specimen	E_d (psi)
unweathered	4.47×10^6
unweathered	4.38×10^6
1-I-C	3.86×10^6
1/4-I-C	3.98×10^6
1-II-B	4.20×10^6
1/4-II-A	4.12×10^6
1-III-B	3.76×10^6
1/4-III-C	4.15×10^6
1-IV-B	4.12×10^6
1/4-IV-B	4.15×10^6
U	2.48×10^6

3.3.2 Second Concrete Batch

The concrete cylinders were exposed to 250 freeze/thaw cycles while emmersed in water. Practically no surface damage was observed after the completion of the freeze/thaw exposure.

The average 28-day compressive strength of this batch of concrete is 4,156psi (the compressive strengths for 4 cylinders are 3207, 4583, 4240 and 4594psi). The measured compressive strength values for selected cylinders and the dynamic modulus values for all cylinders are presented in Table 3.8.

Table 3.8

Dynamic Modulus and Compressive Strength Values for the Second Batch of Concrete

Specimen	Specimen No.	Weight (kg)	Fundamental Transverse Frequency (Hz)	Dynamic Modulus (ksi)	Compressive Strength (psi)
Control (U)	32	12.741	3,910	5,033	7,077
Control (U)	33	12.806	3,900	5,032	
Control (U)	34	12.811	3,870	4,957	7,997
I-1/4-10	28	12.261	3,600	4,106	
I-1/4-2	3	12.119	3,780	4,474	
I-1/4-2	42	12.21	3,660	4,226	
I-1-10	4	12.227	3,670	4,255	
I-1-2	1	12.206	3,680	4,271	
I-1-2	5	12.187	3,770	4,475	5,556
I-1-300	2	12.756	3,950	5,142	
I-1-300	9	12.348	3,940	4,953	
I-1-300	18	11.774	3,530	3,791	4,246
I-1-300	22	12.225	3,900	4,804	
II-1/4-10	35	12.249	3,810	4,594	
II-1/4-2	30	12.33	3,710	4,385	
II-1/4-2	44	12.272	3,750	4,459	
II-1-10	41	12.341	3,790	4,580	
II-1-2	40	12.281	3,780	4,534	6,900
II-1-2	43	12.208	3,960	4,946	
II-1-300	29	12.352	3,740	4,464	
II-1-300	37	12.347	3,950	4,977	6,635
III-1/4-10	16	12.277	3,950	4,949	
III-1/4-2	8	12.281	3,770	4,510	
III-1/4-2	11	12.296	3,930	4,907	
III-1-10	10	12.3	3,860	4,735	
III-1-2	6	12.26	3,930	4,892	5,025
III-1-2	14	12.267	3,890	4,796	
III-1-300	12	12.342	3,900	4,850	
III-1-300	13	12.351	3,800	4,608	4,848
IV-1/4-10	31	12.162	3,820	4,585	
IV-1/4-2	39	12.346	3,700	4,367	
IV-1/4-2	45	12.275	3,800	4,580	
IV-1-10	7	12.25	3,890	4,789	
IV-1-2	36	12.342	3,870	4,776	
IV-1-2	38	12.264	3,880	4,770	6,971
IV-1-300	19	12.237	3,940	4,908	6,688
IV-1-300	24	12.298	3,840	4,685	6,599
IV-1-300	25	12.326	3,800	4,599	
IV-1-300	48	12.261	3,910	4,843	
U-300	15	12.054	3,680	4,218	5,732
U-300	23	12.317	3,770	4,523	5,308
U-300	26	12.333	3,790	4,577	
U-300	27	12.316	3,780	4,547	

3.4 Task 4 - Computer Modeling of Diffusion

3.4.1 Diffusion in Uncoated Concrete

In modeling the diffusion process, the variable altered to yield the optimal fit with the experimental data was the diffusion coefficient, assumed to be a constant for the material. Since the initial moisture concentration was required, it was determined by the method described in Chapter 2. The initial moisture concentration was found to be 0.1894 g/cm^3 or in other words 8.62% of the total mass for a concrete with a unit weight of about 137 lb/ft^3 . This value is similar to reported values, as an excerpt from a table from the "Handbook of Concrete Engineering" (Fintel, 1974) shows below:

Table 3.9
Free Water Values for Saturated Concrete

Free Water	Unit Weight (lb/ft ³)
9.3%	129.3
8.6%	138.6

The mass loss values from the computer program were curve fit using graphing software. The curve fit is of the form

$$y = a_0 + \frac{a_1}{\left[1 + \left(\frac{x}{a_2} \right)^{a_3} \right]} \quad (3.4)$$

From this equation mass loss predictions were calculated that corresponded to the times at which the experimental mass loss measurements were recorded. The resulting two sets of values could then be compared statistically using the sum of least squares and the correlation coefficient. The above steps were repeated until the closest fit

was achieved between the experimental data and the values from the curve fit of the computer program output. The best curve fit correlation coefficient $r = 0.986$ provided an apparent diffusion coefficient for the concrete of $1.0 \times 10^{-6} \text{ cm}^2/\text{s}$ for the duration for which readings were taken (see Figure 3.26).

The obtained diffusion coefficient value is compared to other values found in the literature in Table 3.10.

Table 3.10
Reported Values for Diffusion Coefficient of Concrete

Reference	Diffusion Coefficient (cm^2/s)
Present Study	1.0×10^{-6}
Hughes	1.4×10^{-6}
Lowe et al.	$4.4 \times 10^{-7} - 3.3 \times 10^{-6}$
Penev et al.	$1.16 \times 10^{-6} - 1.16 \times 10^{-3}$
Pickett	2.67×10^{-6}
Sakata	3.47×10^{-6}
Wittmann et al.	$2.3 \times 10^{-7} - 4.8 \times 10^{-6}$

It can be seen from Figure 3.26 that the shape of the predicted percent mass loss vs. time curve does not match the shape of the curve delineated by the data points. In particular, the predicted curve initially underestimates the percent mass loss, then subsequently predicts values higher than the experimental results.

In order to eliminate the possibility of inaccuracies introduced by a mesh that is too coarse, the mesh was made finer, increasing the number of elements from 1,152 to 4,608 (see Figure 3.27). However, this did not significantly affect the results. In fact, the curve fit actually became slightly worse. The correlation coefficient was 0.984, practically the same as before. Thus, there is no point in introducing more elements.

It is obvious that as more and more mass loss data is accumulated, the optimal curve fit will become more shallow, thereby lowering the apparent diffusion coefficient. It would seem at first glance that this non-linear behavior is due to the fact that vapor diffusion in concrete is simply a non-linear process, and that the diffusion coefficient of concrete is not constant. However, this assumes that the drying process is solely being accomplished by the phenomenon of diffusion. This probably is not true.

Figure 3.26

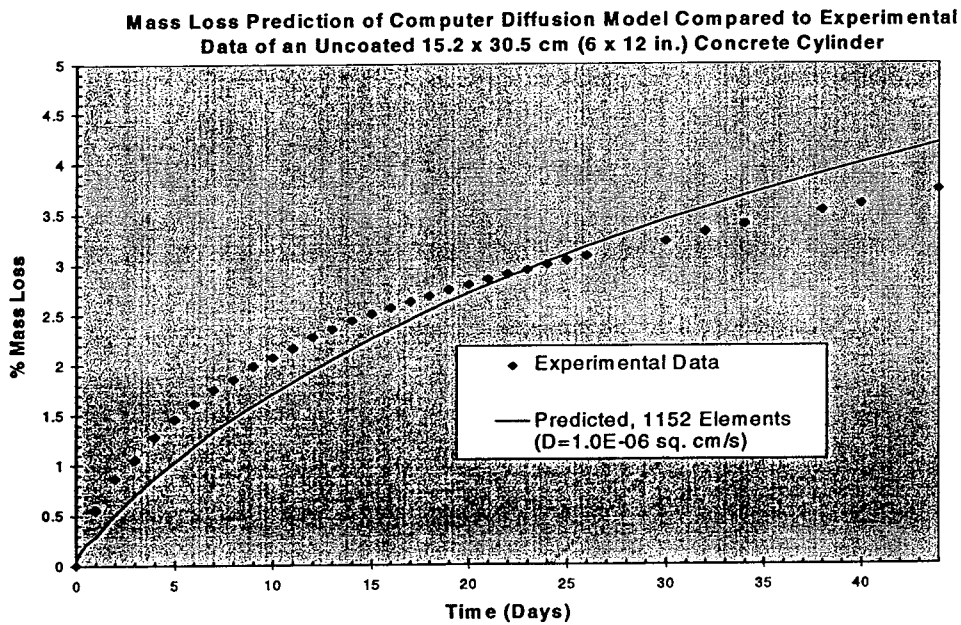
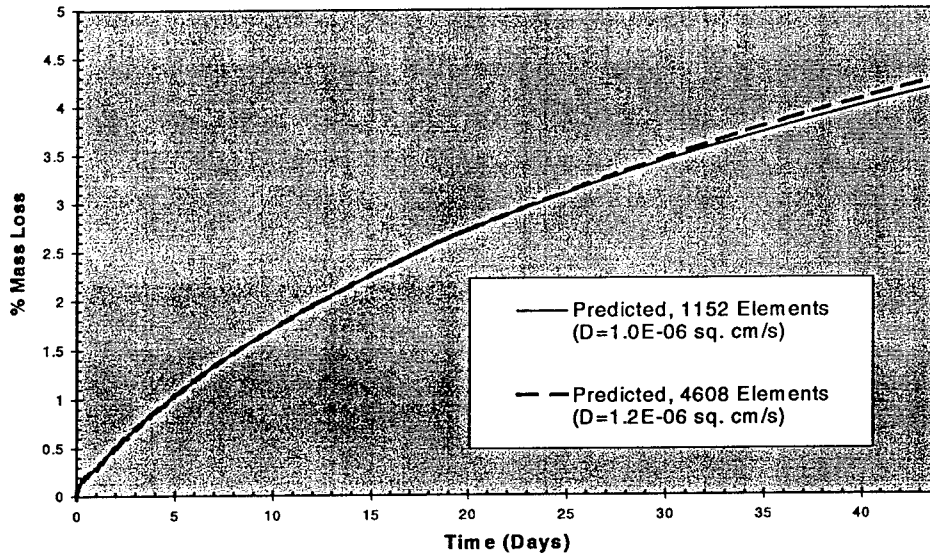


Figure 3.27

Predicted % Mass Loss Values of an Uncoated 15.2 x 30.5 cm Concrete Cylinder for Different Number of Elements



When a porous system is saturated or contains considerable water, the additional transport mechanism of saturated water flow plays an important role in moisture migration (Kropp and Hilsdorf, 1995). In this transport mechanism, capillary action facilitates the movement of condensed water due to surface tension acting in capillaries. Therefore, at high and intermediate moisture concentrations the length of the path traveled by the exiting moisture is shortened, as diffusion is instantaneous across pores and voids filled with water, and moisture migration is dependent on capillary action. Wittman et al. [1988] assert that vapor diffusion becomes a factor only at an RH less than 90%. Even at an intermediate RH, the transport mechanism that dominates in smaller pores is saturated water flow, as the smaller pores are still filled with water in liquid form. Thus, the diffusion coefficient determined from a drying curve is artificially inflated, and this is the reason why it overestimates mass loss

values in the latter half of the curve. The lowering of the apparent moisture diffusion coefficient that occurs with the passage of time will increase the accuracy of the coefficient prediction, i.e., as $t \rightarrow \infty$ the apparent diffusion coefficient will approach the true diffusion coefficient. Stated another way, as a larger portion of the curve represents concrete at lower RH, the diffusion process will be better represented. In other words, the drying process will be indicative solely of the diffusion of moisture, and not diffusion combined with other transport mechanisms. It would then seem that the true vapor diffusion coefficient can only be determined at low moisture conditions. In addition, this casts doubt on the veracity of the various schemes evinced by the bulk of the articles in the literature dealing with moisture diffusion in concrete. Thus, the upper bound values of the ranges for the diffusion coefficient reported in the literature (Table 3.9) appear to be fictitious. The diffusion coefficient is made to be a function of moisture concentration, time, and space, and a variety of creative and contrived functions are crafted to make the theory fit the data (see Section 1.3.2). In fact it is the assumption that diffusion is the only phenomenon that figures in drying that should be questioned, and not whether the diffusion behavior of concrete - an intrinsic property if there ever was one (Kropp and Hilsdorf, 1995) - changes due to the availability of the material diffusing through it!

In short, while nonlinear diffusion theory may predict the moisture concentration in concrete more accurately, it may be just as useful - and more rational

- to formulate a model that uses capillary action in conjunction with diffusion to project the moisture content within concrete at a given time.

3.4.2 Diffusion in Coated Concrete

Nevertheless, it can be seen that for coatings, linear diffusion theory performs reasonably well in predicting moisture migration. The introduction of a coating improves the accuracy of the theory, and the more impermeable the coating is the better the curve fit becomes. This is probably because the flattened drying curve that results from the additional restriction of moisture flow furnished by the coating agrees more with the shape of the curve that arises from linear diffusion theory.

Table 3.11 reports the average thickness found for each coating, as determined by the method described in section 2.3. These values were used in modeling the coating for the computer program. The curve fit for each coating is shown in Figures 3.28 - 3.31. The correlation coefficient for Figure 3.28 is 0.992. However, as noted above, the correlation coefficients for the more impermeable epoxy coatings were at least 0.999. The apparent diffusion coefficients are also tabulated in Table 3.11. Nguyen et al. [1995] found that for a pigmented, water-reducible epoxy the apparent D with respect to water was $3.2 \times 10^{-8} \text{ cm}^2/\text{s}$, and for a clear, solvent-free epoxy $D = 1.0 \times 10^{-8} \text{ cm}^2/\text{s}$. This indicates that the computer program is useful in regard to modeling moisture flow out of coated concrete.

Table 3.11
Average Coating Thickness and Diffusion Coefficient

Coating Type	Thickness (μm)	Apparent D (cm^2/s)
I	1560	1.0×10^{-7}
II	80	0.6×10^{-8}
III	76	1.1×10^{-8}
IV	73	1.0×10^{-8}

Figure 3.28

**Mass Loss Prediction Compared to Experimental Data
 from Specimen Coated with Coating I**

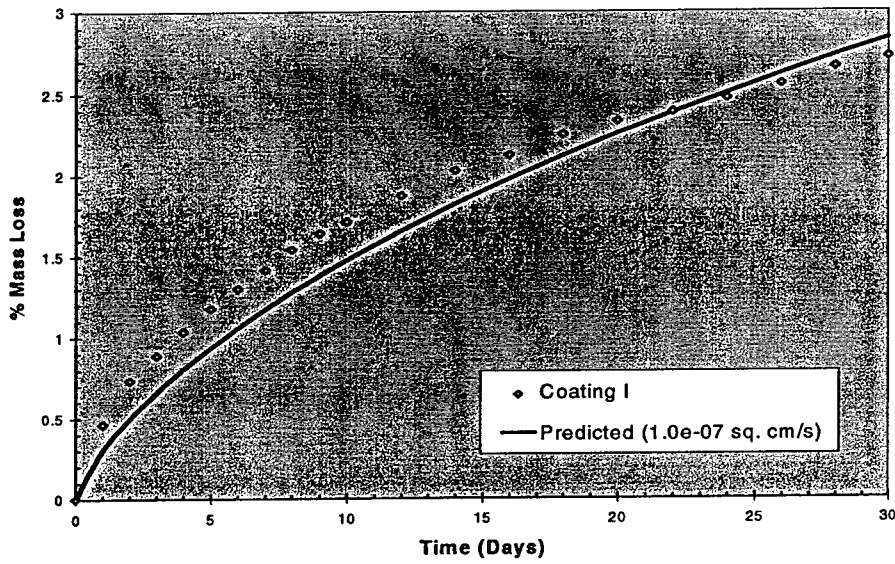


Figure 3.29

Mass Loss Prediction Compared to Experimental Data from Specimen Coated with Coating II

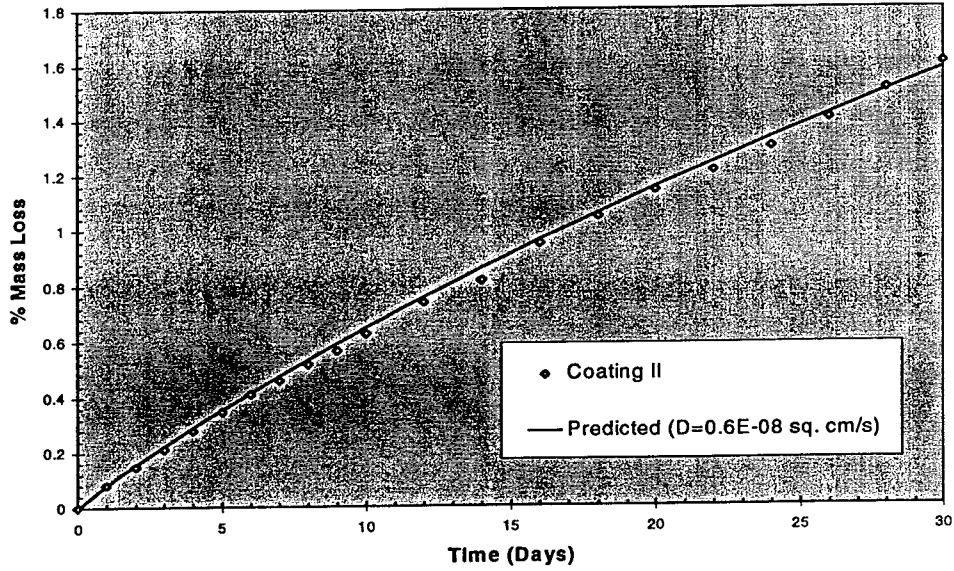


Figure 3.30

Mass Loss Prediction Compared to Experimental Data from Specimen Coated with Coating III

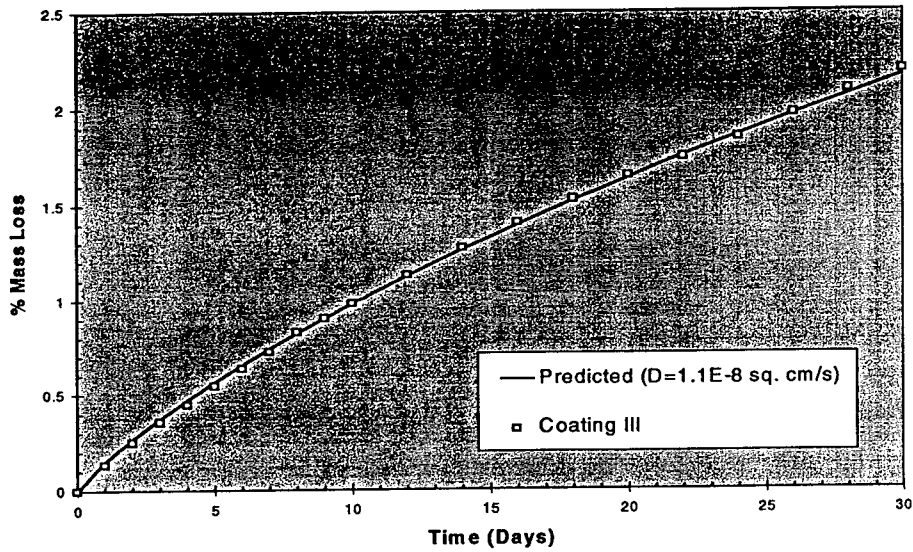
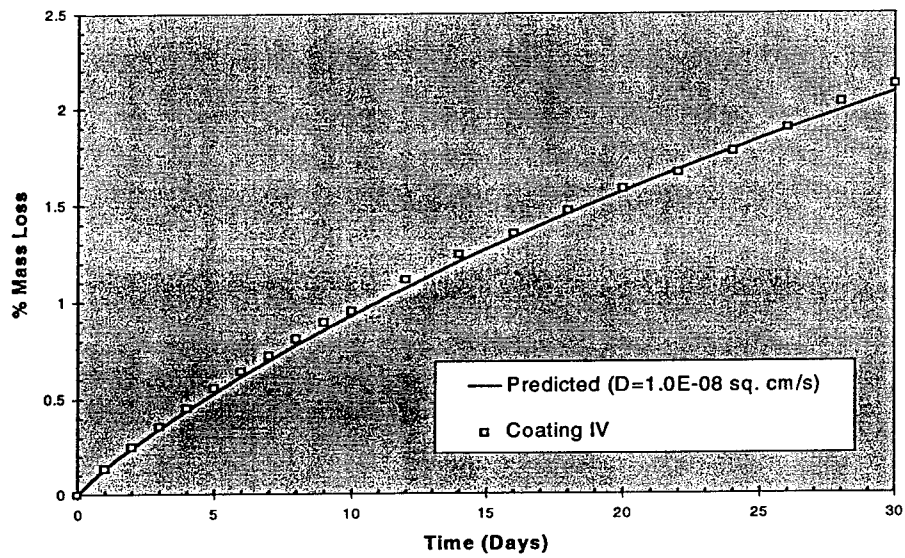


Figure 3.31

Mass Loss Prediction Compared to Experimental Data
from Specimen Coated with Coating IV



CHAPTER FOUR

CONCLUSIONS

4.1 Summary of Significant Observations and Conclusions

For cylindrical specimens composed of Class C structural concrete and coated with Coatings I, II and III, it was observed that the encapsulation of moisture did not result in any discernible deterioration after 150 freeze/thaw cycles in air where the concrete temperature ranged from +1.5°C to -1.5°C. In fact, the compressive strength of sealed "weathered" specimens was generally higher than the compressive strength of uncoated specimens that were not exposed to freeze/thaw. However, specimens that were permitted drying time before coating application displayed higher strengths than those that were coated immediately after the completion of curing. Compressive strength was also found to be higher in concrete cylinders cured at 100% RH than in those that were not.

Significant surface damage was observed on specimens after 60 freeze/thaw cycles in water. Also, the dynamic modulus of elasticity decreased. Nevertheless, even here it was evident that not only did the concrete coatings minimize freeze/thaw damage, but they improved compressive strength compared to specimens that were not coated at all. In addition, it was observed that specimens that were only partially coated did not exhibit improved freeze/thaw resistance. Specimens that were cured while covered with wet burlap and plastic sheeting at room temperature had less

spalling than specimens cured in an environment with 100% RH and a continuous temperature of 70°F.

For the sealants and the concrete used during the course of this project, the following conclusions can be drawn from the results of the research conducted:

- a. Encapsulation of moisture is not an important factor in the contribution of freeze/thaw degradation in concrete;
- b. In general, sealing concrete not only mitigates the damage caused by freezing and thawing, but also increases the compressive strength of concrete;
- c. One can readily and reliably determine the moisture concentration in concrete with the aid of a device that measures relative humidity;
- d. No benefits are gained by leaving portions of the surface area of concrete uncoated;
- e. Curing concrete in an environment that allows partial drying to periodically occur results in less surface damage to concrete than a curing environment that keeps the concrete continually saturated;
- f. Diffusion theory alone is not sufficient to describe the movement of water in concrete;
- g. Nevertheless, a diffusion-based computer model can adequately model the migration of moisture in concrete that has been coated.

4.2 Suggestions for Future Work

In order to understand the relationships between concrete microstructure and transport properties, more experimental data of transport properties are needed on numerous samples of different grades of concrete. To determine whether a given analytical property is useful, or if a given computer simulation is correct, the degree of saturation and porosity of the cement paste, the volume and size distribution of the aggregates, the width of the interfacial zones, and the values of the pertinent transport coefficients for the matrix and the aggregate materials of a concrete sample must be known.

In particular, the theoretical relationships between coefficients of different transport phenomena have hardly been studied, and there is little, if any, experimental data. An attempt should be made to create experimental procedures that can study transport phenomena separately. Then a mathematical model can be formulated that super-imposes the effects of all the relevant flow mechanisms.

Undoubtedly one of the main parameters that will influence the predictions of any such model is the air-void system, for as drying proceeds diffusion will become the dominant behavior in larger pores that have been at least partially emptied of liquid water, while saturated water flow will still persist in smaller pores that are filled with water due to capillary action. Therefore, not only must parameters such as the air-void frequency, spacing factor, paste-air ratio, and specific surface be calculated (as per ASTM C 457), but the distribution of the various sizes of potential moisture

pathways must also be determined if one is to be truly able to gain an understanding of moisture flow.

In addition, as noted in section 1.3.1, current freeze/thaw tests do not really duplicate conditions in the field. The mechanism of ice accretion, for example, is not accounted for when studying freeze/thaw damage, probably due to the intrinsically time-consuming nature of the process. Nevertheless, it behooves the civil engineering community to evaluate the severity of the effects of this mechanism.

If transport mechanisms through concrete are not comprehensively understood, the situation in regard to coatings is even more marked by ignorance. Study of the coating/concrete interface should be conducted, and study of a given coating's chemical structure probably should be taken into consideration. Mechanisms of coating failure such as blistering, pinholing, cracking, and detachment (Hewlett, 1990) also need to be understood, not merely identified. Furthermore, a standard for rating the level of surface quality should be devised, as surface preparation is of major importance to coating performance.

APPENDIX A

REFERENCES

- American Society for Testing and Materials. (1992). "C 39 Standard Test Method for Compressive Strength of Cylindrical Concrete Specimens," *Annual Book of ASTM Standards*, Philadelphia, PA, Vol. 04.02, 17-21.
- American Society for Testing and Materials. (1992). "C 192 Practice for Making and Curing Concrete Test Specimens in the Laboratory," *Annual Book of ASTM Standards*, Philadelphia, PA, Vol. 04.02, 113-119.
- American Society for Testing and Materials. (1992). "C 215 Standard Test Method for Fundamental Transverse, Longitudinal, and Torsional Frequencies of Concrete Specimens," *Annual Book of ASTM Standards*, Philadelphia, PA, Vol. 04.02, 124-128.
- American Society for Testing and Materials. (1982). "C 457 Standard Practice for Microscopical Determination of Air-Void Content and Parameters of the Air-Void System in Hardened Concrete," *Annual Book of ASTM Standards*, Philadelphia, PA, Vol. 04.02, 229-240.
- American Society for Testing and Materials. (1992). "C 666 Standard Test Method for Resistance of Concrete to Rapid Freezing and Thawing," *Annual Book of ASTM Standards*, Philadelphia, PA, Vol. 04.02, 320-324.
- American Society for Testing and Materials. (1984). "C 671 Standard Test Method for Critical Dilation of Concrete Specimens Subjected to Freezing," *Annual Book of ASTM Standards*, Philadelphia, PA, Vol. 04.02, 334-338.
- American Society for Testing and Materials. (1984). "C 682 Standard Practice for Evaluation of Frost Resistance of Coarse Aggregates in Air-Entrained Concrete by Critical Dilation Procedures," *Annual Book of ASTM Standards*, Philadelphia, PA, Vol. 04.02, 342-345.
- EarthInfo, Inc. (1995). *EarthInfo CD-ROM Reference Manual*, Boulder, Colorado.
- State of Ohio Department of Transportation. (1989). *Construction and Material Specifications*, 451.03-511.09.
- Aarre, T. (1995). "Influence of measurement Technique on the Air-Void Structure of Hardened Concrete," *ACI Materials Journal*, Vol. 92, No. 6, 599-604.

- Aldinger, T.I. (1991). "Technical Specifications for Concrete Coatings Work," *Materials Performance*, Vol. 30, 36-41.
- Bakharev, T. and Struble, L.J. (1995). "Microstructural Features of Freeze-Thaw Deterioration of Concrete," *Microstructure of Cement-Based Systems/Bonding and Interfaces in Cementitious Materials*, Materials Research Society, *Symposium Proceedings*, Vol. 370, 83-88.
- Bazant, Z.P., Chern, J., Rosenberg, A.M., and Gaidis, J.M. (1988). "Mathematical Model for Freeze-Thaw Durability of Concrete," *Journal of the American Ceramic Society*, Vol. 71, 776-783.
- Bazant, Z.P. and Najjar, L.J. (1971). "Drying Concrete as a Nonlinear Diffusion Problem," *Cement and Concrete Research*, Vol. 1, 461-473.
- Blight, G.E. (1990). "Can Concrete Structures Be Waterproofed to Inhibit ASR?," *Protection of Concrete, Proceedings of the International Conference*, Chapman & Hill, London, Great Britain, 223-232.
- Cady, P.D. (1969). *Mechanisms of Frost Destruction in Concrete*, Ph.D. Thesis, Pennsylvania State University, University Park, PA.
- Carlson, R.W. (1937). "Drying Shrinkage of Large Concrete Members," *American Concrete Institute Journal*, Vol. 8, No. 3, 327-336.
- Cook, H.K. (1952). "Experimental Exposure of Concrete to Natural Weathering in Marine Locations," *Proceedings, ASTM*, V. 52, 1169-1180.
- Cordon, W.A. (1966). *Freezing and Thawing in Concrete - Mechanisms and Control*, ACI Monograph No. 3, Iowa State University Press, Detroit, 99pp.
- Crank, J. (1956). *The Mathematics of Diffusion*, Oxford University Press, London, Great Britain.
- Detwiler, R., Dalgleish, B.J., and Williamson, R.B. (1989). "Assessing the Durability of Concrete in Freezing and Thawing," *ACI Materials Journal*, January-February, 29-35.

- Fagerlund, G. (1977). "The Critical Degree of Saturation Method of Assessing the Freeze/Thaw Resistance of Concrete," *Materials and Structures, Research and Testing*, Vol. 10, No. 58. 217-229.
- Fera, J.D. (1991). "Laboratory Evaluation of Concrete Sealers for Vertical Highway Structures," *Research Report FHWA-RI-90-1*, Rhode Island Department of Transportation, Providence, RI.
- Fintel, M. (1974). *Handbook of Concrete Engineering*, Van Nostrand Reinhold Company, New York.
- Foscante, R.E., and Kline, H.H. (1988). "Coating Concrete - An Overview," *Materials Performance*, Vol. 27, 34-36.
- Fourier, J.B. (1822). *Oeuvres de Fourier*, Gauthier-Villars et fils, Paris, France.
- Fukute, T. and Hamada, H. (1990) "Surface Coatings for Improving Performance of Concrete Under Marine Environments," *Protection of Concrete, Proceedings of the International Conference*, Chapman & Hill, London, Great Britain, 316-330.
- Garcia, A.M., Alonso, C. and Andrade, C. (1990) "Evaluation of the Resistance of Concrete Coatings Against Carbonation and Water Penetration," *Protection of Concrete, Proceedings of the International Conference*, Chapman & Hill, London, Great Britain, 233-243.
- Harwood, P.C. (1990). "Surface Coatings - Specification Criteria," *Protection of Concrete, Proceedings of the International Conference*, Chapman & Hill, London, Great Britain, 201-210.
- Helmuth, R.A. (1960). "Capillary Size Restrictions on Ice Formation in Hardened Portland Cement Pastes," *Proceedings of the Fourth International Symposium on Chemistry of Cement, Paper VI-S2*, U.S. National Bureau of Standards, 855-869.
- Hewlett, P.C. (1990). "Methods of Protecting Concrete - Coatings and Linings," *Protection of Concrete, Proceedings of the International Conference*, Chapman & Hill, London, Great Britain, 105-134.
- Hughes, B.P., Lowe, I.R.G., and Walker, J. (1966). "The Diffusion of Water in Concrete at Temperatures Between 50 and 95°C," *British Journal of Applied Physics*, Vol. 17, 1545-1552.

- Kropp, J. and Hilsdorf, H.K. (1995). *Performance Criteria for Concrete Durability, RILEM Report 12*, Chapman & Hall, New York.
- Leake, W. (1993). "Encapsulation of Concrete," *Inter-Office Communication*, Ohio Department of Transportation, District 12, Garfield Heights, OH, 2 pp.
- Leeming, M. (1990). "Surface Treatments for the Protection of Concrete," *Protection of Concrete, Proceedings of the International Conference*, Chapman & Hill, London, Great Britain, 135-148.
- Lowe, I.R.G., Hughes, B.P., and Walker, J. (1971). "The Diffusion of Water in Concrete at 30°C," *Cement and Concrete Research*, Vol. 1, 547-557.
- McGill, L.P. and Humpage, M. (1990). "Prolonging the Life of Reinforced Concrete Structures by Surface Treatment," *Protection of Concrete, Proceedings of the International Conference*, Chapman & Hill, London, Great Britain, 191-200.
- Mensi, R., Acker, P., and Attolou, A. (1988). "*Sechage du Beton: Analyse et Modelisation*," *Materials and Structures*, Vol. 21, 3-12.
- Miao, B. (1988). *Effets Mecaniques dus au Retrait de Dessiccation du Beton*, Doctoral Thesis, Ecole Nationale des Ponts & Chaussees de Paris, Paris, France.
- Mindess, S. and Young, F. (1981). *Concrete*, Prentice-Hall, Inc., Englewood Cliffs.
- Neville, A.M. (1963). *Properties of Concrete*, Pitman Publishing Corporation, New York.
- Nguyen, T., Bentz, D. and Byrd, E. (1995). "Method for Measuring Water Diffusion in a Coating Applied to a Substrate," *Journal of Coatings Technology*, Vol. 67, No. 844, 37-46.
- Odler, I. and Barthold, H. (1989). "Investigations on the Water Vapor Permeability of Cementitious Materials," *Pore Structure and Permeability of Cementitious Materials, Materials Research Society, Symposium Proceedings*, Vol. 137, 215-222.
- Penev, D., and Kawamura, M. (1991). "Moisture Diffusion in Soil-Cement Mixtures and Compacted Lean Concrete," *Cement and Concrete Research*, Vol. 21, 137-146.

- Pickett, G. (1946). "Shrinkage Stresses in Concrete," *Journal of the American Concrete Institute*, Vol. 17, No. 3, 165-204.
- Pihlajavaara, S.E. (1965). *On the Main Features and Methods of Investigation of Drying and Related Phenomena in Concrete*, Ph.D. Thesis, Publ. No. 100, State Institute for Technical Research, Helsinki, Finland.
- Pihlajavaara, S.E., and Vaisanen, J. (1965). "Numerical Solution of Diffusion Equation with Diffusivity Concentration Dependent," Publ. No. 87, State Institute for Technical Research, Helsinki, Finland.
- Powers, T.C. (1949). "Air Requirement of Frost-Resistant Concrete," *Proceedings, Highway Research Board*, Vol. 29, 184-211.
- Reedy, G. (1986). "Deck Epoxies, Sealants Not Advised for Substructure," *Roads & Bridges*, August, 29-32.
- Rewerts, T.L. (1993). "Beware of Internal Moisture When Coating Concrete," *Concrete Construction*, June, 421-425.
- Sakata, K. (1983). "A Study of Moisture Diffusion in Drying and Drying Shrinkage in Concrete," *Cement and Concrete Research*, Vol. 13, 216-224.
- Sandstrom, M. (1991). "Air-Void Distribution in Concrete," *Third Euroseminar on Microscopy Applied to Building Materials*, Barcelona, Spain, 1-7.
- Scheaffer, R.L., and McClave, J.T. (1986). *Probability and Statistics for Engineers*, PWS Publishers, Boston.
- Shanati, S., Ellis, N.S., and Randall, T.J. (1995) "Coupled Diffusion and Stress by the Finite Element Method," *Applied Mathematical Modelling*, Vol. 19, No. 2, 87-94.
- Sherwood, T.K. (1929). "The Drying of Solids," *Industrial and Engineering Chemistry*, Vol. 21, No. 10, 976-980.
- Sommer, H. (1979). "Precision of the Microscopical Determination of the Air-Void System in Hardened Concrete," *Cement, Concrete, and Aggregates*, Vol. 1, No. 2, 49-55.
- Swamy, R.N. and Tanikawa, S. (1990). "Surface Coatings to Preserve Concrete Durability," *Protection of Concrete, Proceedings of the International Conference*, Chapman & Hill, London, Great Britain, 149-165.

Terro, B.S. and Hughes, D.C. (1990). "Surface Treatment of Hydrated Cement Paste Using 'Xypex'", *Protection of Concrete, Proceedings of the International Conference*, Chapman & Hill, London, Great Britain, 303-315.

Weyers, R.E., Zemajtis, J. and Drumm, R.O. (1995). "Service Lives of Concrete Sealers," *Management and Maintenance of Bridge Structures, Transportation Research Record 1490*, July, 54-59.

Wittman, F.H., Roelfstra, P.E., and Kamp, C.L. (1988) "Drying of Concrete: an Application of the 3L-Approach," *Nuclear Engineering and Design*, Vol.105, 185-198.

Wittman, X., Sadouki, H. and Wittman, F.H. (1989). "Numerical Evaluation of Drying Test Data," *Transactions Tenth International Conference of Structural Mechanics in Reactor Technology (SMIRT)*, Vol. Q, 71-79.

Zemajtis, J. and Weyers, R.E. (1995). "Service Life Evaluation of Concrete Surface Coatings," *Management and Maintenance of Bridge Structures, Transportation Research Record 1490*, July, 67-74.